actuators

MDPI

Article

Low-Frequency Micro-Vibration Attenuation of Slender Cantilever Precision Positioning Actuators Using Particle Damping

Baichao Wang [1,*], Hao Wang [1,*], Chao Zhang [2], Xuanyu Jin [1], Haonan Dai [1], Litong Zhang [1] and Mingyang Liu [3]

[1] School of Mechanical and Electrical Engineering, Changchun University of Science and Technology, No. 7089, Satellite Road, Chaoyang District, Changchun 130013, China; 2024100493@mails.cust.edu.cn (X.J.); 2024100529@mails.cust.edu.cn (H.D.); zhanglitong@cust.edu.cn (L.Z.)
[2] Shanghai Institute of Optics and Fine Mechanics, Chinese Academy of Sciences, No. 390 Qinghe Road, Jiading District, Shanghai 201800, China; zhangchao7125@126.com
[3] Dalian University of Technology, No. 2, Linggong Road, Ganjingzi District, Dalian 116024, China; 32506183@mail.dlut.edu.cn
* Correspondence: bcwang@cust.edu.cn (B.W.); 2024200140@mails.cust.edu.cn (H.W.)

Abstract

Slender cantilever precision positioning actuators are highly susceptible to ambient low-frequency micro-vibrations, which severely deteriorate dynamic positioning accuracy and operational stability. To address this challenge, this paper proposes a passive vibration attenuation method utilizing a customized partitioned particle damper. A micro-vibration-adapted discrete element method (DEM) coupled dynamic model is established to quantitatively characterize the underlying multi-mechanism energy dissipation driven by micro-slip friction and weak inelastic collisions. Through systematic numerical parametric analysis and physical experimentation, the optimal damper configuration is identified. Experimental results rigorously demonstrate that the optimized particle damper effectively suppresses broadband micro-vibrations (10–100 Hz), achieving a maximum steady-state vibration damping efficiency of 63.24% and a transient peak acceleration attenuation of 67.5% at the cantilever tip. This work provides a highly compact, energy-free, and robust structural vibration suppression strategy, demonstrating significant potential for application in high-precision actuation systems.

Keywords: particle damping; slender cantilever precision actuator; discrete element method; low-frequency micro-vibration attenuation; structural dynamic stability

Check for updates

Academic Editor: Eihab M. Abdel-Rahman

Received: 27 June 2026
Revised: 26 July 2026
Accepted: 31 July 2026
Published: 3 August 2026

Copyright: © 2026 by the authors. Licensee MDPI, Basel, Switzerland. This article is an open access article distributed under the terms and conditions of the Creative Commons Attribution (CC BY) license.

1. Introduction

With the rapid advancement of high-end precision manufacturing and aerospace detection technologies, including ultra-precision semiconductor processing and high-resolution aerospace observation, modern precision actuation and positioning systems are evolving toward ultra-high precision, miniaturization, and high integration [1,2]. Slender cantilever positioning actuators, as typical flexible precision actuation components, have been extensively adopted in limited-space precision positioning scenarios owing to their prominent merits of lightweight structure, superior spatial accessibility, and flexible motion characteristics [3,4]. Nevertheless, the inherent structural features of high slenderness ratio, low structural stiffness, and weak inherent damping render such cantilever actuators highly sensitive to subtle external ambient excitations [5]. The induced low-frequency micro-vibrations will directly deteriorate the structural stability, terminal pose accuracy, and

operational reliability of precision positioning actuators, becoming a critical bottleneck restricting the performance improvement of high-precision actuation systems. Therefore, it is imperative to develop low-frequency micro-vibration attenuation strategies tailored to slender cantilever precision positioning actuators to enhance their dynamic anti-interference capability and positioning accuracy in complex service environments.

Aiming at the micro-vibration suppression challenges of flexible cantilever precision actuation structures, numerous studies have been conducted on dynamic modeling, vibration control strategies, and structural optimization of cantilever systems. Kumar et al. [6] proposed an adaptive relay feedback self-excitation approach to characterize the steady-state dynamic response of cantilever structures, verifying that the distribution of lumped mass and damping parameters significantly affects the accuracy of dynamic modeling. Verma et al. [7,8] employed viscoelastic materials to suppress structural vibration of cantilever beams with tip masses and investigated the transient dynamic regulation performance of different viscoelastic parameter configurations. However, viscoelastic material-based vibration mitigation methods exhibit strong frequency dependence, limited suppression capacity for low-amplitude micro-vibrations, and poor environmental adaptability, restricting their application in high-precision actuation scenarios. Qian et al. [9,10] designed a nonlinear spring-inerter-damper energy absorber for vibration control of single-supported beam structures and experimentally validated its vibration reduction effectiveness. Song et al. [11,12] exploited the stress and strain sensing characteristics of piezoelectric materials to realize cantilever vibration suppression and further improved the low-frequency vibration attenuation performance via hybrid active–passive control strategies. While these methods can be effective, tuned mass damper (TMD) techniques rely heavily on precise frequency matching with the primary structure, while active and hybrid control systems require additional external power supply and control units, which inevitably increase the structural complexity, weight, and cost of precision actuation equipment. Amir et al. [13,14] proposed a cross-section-based topological optimization method for beam structures, which improves the fundamental frequency and reduces structural weight and elastic modulus. Nevertheless, structural topology optimization involves complex modeling and computationally intensive calculations, and the optimized configurations often suffer from poor engineering manufacturability and low practicability in miniature precision actuators.

In summary, existing vibration suppression methods for cantilever structures mainly focus on improving structural stiffness and inherent damping. However, most traditional techniques require invasive structural modifications to original precision actuators or additional auxiliary control modules, which pose challenges to the lightweight and integrated design requirements of modern high-precision positioning equipment. As a novel passive vibration control technology [15–18], particle damping (PD) possesses unique advantages of minimal structural invasion, simple configuration, easy integration, and energy-free operation, which is suitable for the requirements of precision actuation systems. The vibration energy dissipation of particle damping is primarily realized through the collision and friction damping effects of internal particle media [19–22], and it has been widely verified in civil engineering, mechanical equipment, and aerospace structures. Zhao et al. [23] adopted particle dampers to suppress train-induced structural vibration and achieved effective vertical acceleration attenuation in specific bandgaps. Xiao et al. [24] applied particle damping technology to gear vibration control, verifying its superior stability and reliability in mechanical vibration suppression. Niedermeyer et al. [25] introduced particle damping into aero-engine compressor blade vibration reduction and effectively improved the structural damping performance of blade components. Although particle damping has demonstrated excellent applicability and reliability in various macro-scale vibration

suppression fields, systematic research on its low-frequency micro-vibration suppression performance for slender cantilever precision actuators remains insufficient. Exploring the application of particle damping in low-frequency micro-vibration attenuation of flexible cantilever positioning actuators could contribute to the field of passive vibration control for precision actuation structures and provide an innovative engineering solution for micro-vibration control of high-precision positioning systems.

Different from conventional continuum vibration damping methods, particle damping involves discrete particle collision and friction coupling behavior, which cannot be accurately analyzed by traditional continuum mechanics theories. The discrete element method (DEM), first proposed by Cundall and Strack in 1979 for geomechanics analysis [26–28], provides an effective numerical tool for characterizing discrete particle damping behavior. Rongong et al. [29] experimentally investigated the damping characteristics of particle-damped single-degree-of-freedom systems and summarized their medium- and high-frequency vibration attenuation performance. Lu et al. [28] analyzed the damping mechanism under free attenuation, steady-state random excitation, and unsteady excitation conditions and proposed the effective momentum exchange theory to explain the energy dissipation principle of particle systems. Nevertheless, the standard DEM based on Newton's second law fails to directly quantify the micro-vibration attenuation effect and equivalent damping characteristics of particle damping structures [30,31]. While previous studies have successfully applied particle damping to macro-scale structures such as conventional cantilever beams, aero-engine compressor blades, and gears, its implementation in ultra-precision cantilever positioning mechanisms faces fundamentally different constraints. In this specific scenario, a comparative analysis reveals the limitations of other mainstream vibration suppression methods. Active vibration control systems, such as piezoelectric or electromagnetic actuators, offer high adaptability but introduce inevitable thermal deformations and electrical noise, which can be fatal to sub-micron terminal positioning accuracy. Among passive methods, Tuned Mass Dampers (TMDs) are limited by their narrow effective frequency bandwidth and high sensitivity to detuning, making them inadequate for complex broadband environmental micro-vibrations. Furthermore, traditional viscous fluid dampers pose a severe risk of fluid leakage, which is strictly prohibited in clean and highly sensitive precision manufacturing environments. In stark contrast, the particle damping methodology provides a unique set of advantages for this scenario: it is completely passive (generating zero thermal/electrical disturbances), possesses inherent broadband energy dissipation characteristics, and operates strictly dry (eliminating contamination risks). By further proposing a customized partitioned cavity design, this work overcomes the traditional horizontal gravity agglomeration issue, innovatively adapting this robust damping mechanism to the strict requirements of precision cantilever actuators.

By systematically summarizing and comparing the existing particle damping research on cantilever beams, blades, and precision structures, three core unresolved scientific and engineering problems are clarified:

1. Scale mismatch: Previous particle-damping studies primarily address macro-scale vibration suppression, lacking targeted solutions for the low-frequency and ultra-small-amplitude micro-vibrations inherent to slender cantilever precision positioning actuators.
2. Mechanism divergence: The conventional assumption that particle damping is dominated by collision energy is invalid for precision structures. Under micro-vibration conditions, the actual energy dissipation is jointly governed by micro-slip friction and quasi-static hysteresis extrusion, with micro-collisions playing only a minor role.
3. Methodological limitation: The standard Discrete Element Method (DEM) fails to directly quantify micro-vibration attenuation and equivalent damping characteristics.

This necessitates a refined DEM model incorporating a correction coefficient λ_m to accurately characterize weak elastic contact and micro-slip friction without assuming severe particle jumping or large-scale sliding.

To address this gap, this paper establishes a coupled numerical model integrating discrete element method and multi-body dynamics, which enables quantitative calculation and analysis of structural vibration response variation, equivalent damping characteristics, and energy dissipation mechanism of particle-damped cantilever precision actuators. The proposed method possesses three core innovations:

1. A micro-vibration-adapted discrete element model for particle damping systems is established, introducing two novel correction coefficients—the micro-vibration contact damping correction coefficient λ_m and the rotational correction coefficient η_m —which modify the conventional spring-damper contact model to accurately capture the weak elastic collision and micro-slip friction behaviors under ultra-low-amplitude excitation (10^{-5} g–10^{-3} g), overcoming the modeling deficiency of traditional DEM in precision actuation micro-vibration scenarios.
2. A multi-mechanism energy dissipation model under micro-vibration conditions is quantitatively established, decomposing the total energy dissipation into three components: micro-slip friction, quasi-static hysteresis extrusion, and micro-collision. This model clarifies that, unlike conventional macro-vibration damping, the energy dissipation in low-frequency micro-vibrations is jointly dominated by micro-slip friction and hysteresis, providing a theoretical basis for parameter optimization.
3. A systematic parametric analysis and experimental verification strategy is conducted to determine the optimal coupling configuration of particle size and filling ratio. The identified optimal configuration (1.4 mm stainless steel particle size +92% filling ratio) achieves a 63.24% vibration damping rate and 67.5% peak acceleration reduction, with validated broadband suppression performance across the 10–100 Hz frequency range and 72% attenuation at the first-order resonance (70 Hz), confirming the engineering applicability of the proposed method for high-precision positioning systems.

The vibration attenuation efficiency of particle damping is highly sensitive to multiple structural and physical parameters, including particle diameter, material properties, surface roughness, recovery coefficient, and damper filling ratio [32]. This paper systematically investigates the influence of key particle damping parameters on the low-frequency micro-vibration dynamic response of slender cantilever precision positioning actuators. The organizational structure of this paper is arranged as follows: Section 2 conducts dynamic modeling and modal analysis of the slender cantilever positioning actuator to identify its dominant vibration modes and low-frequency vibration characteristics. Section 3 establishes a coupled dynamic model of the cantilever actuator and particle damper based on DEM and elaborates the energy dissipation mechanism of particle collision and friction under low-frequency micro-vibration conditions. In Section 4, parametric analysis is performed to explore the effects of particle diameter and filling ratio on energy dissipation performance, and the optimal damper configuration scheme is determined. Section 5 constructs a physical experimental platform for cantilever micro-vibration tests to verify the parametric damping performance and low-frequency suppression effect of the optimized particle damper. Finally, Section 6 summarizes the research conclusions and engineering implications.

2. Dynamic Performance Analysis of Slender Cantilever Precision Positioning Actuator

To clarify the inherent vibration characteristics and low-frequency micro-vibration generation mechanism of the slender cantilever precision positioning actuator, this sec-

tion conducts structural dynamic modeling, finite element modal analysis, and vibration transmission mechanism analysis. The inherent modal parameters, dominant vibration modes, and structural dynamic stiffness distribution of the cantilever actuator are obtained. Furthermore, the external micro-vibration excitation sources and structural vibration transmission paths in practical service environments are analyzed. The analysis results provide a theoretical basis and structural optimization guidance for the subsequent parameter design and layout scheme of particle dampers for low-frequency micro-vibration attenuation.

2.1. Model Establishment and Modal Analysis

In this study, a typical slender cantilever precision positioning actuator widely used in limited-space high-precision positioning scenarios is taken as the research object. A three-dimensional geometric simplified model of the cantilever structure is established, with overall structural dimensions of 1500 mm × 100 mm × 150 mm and a wall thickness of 10 mm. To intuitively display the internal hollow structure of the workpiece, a detailed sectional view is provided. The structural material is 6061 aluminum alloy, which features low density, high specific stiffness, and excellent processing manufacturability, meeting the lightweight and high-stability design requirements of precision actuators. The key material mechanical parameters are set as follows: density of 2.7 g/cm^3, elastic modulus of 69 GPa, and Poisson's ratio of 0.33.

To acquire the low-order inherent modal frequencies and corresponding mode shapes that dominate the low-frequency dynamic response of the slender cantilever actuator, finite element-based modal analysis is carried out via ANSYS Workbench 2021 R1. A hexahedron-dominated meshing strategy is adopted to ensure calculation accuracy and mesh quality, and the SOLID186 structural solid element is selected for mesh discretization. The final finite element model contains 110,058 nodes and 36,186 elements.

To verify the adequacy of the selected mesh density, a systematic mesh convergence study was performed. The mesh was progressively refined across five levels, and the first-order natural frequency was monitored as the convergence criterion. As summarized in Table 1, the relative change in the first natural frequency diminishes to 0.54% when the mesh is refined from the Medium (26,148 elements) to the Fine (36,186 elements) level, and further refinement to 48,520 elements yields a negligible change of 0.06%. The Fine mesh configuration was therefore adopted for all subsequent analyses, ensuring computational accuracy while maintaining efficiency. The established structural geometric model and meshing configuration are demonstrated in Figure 1.

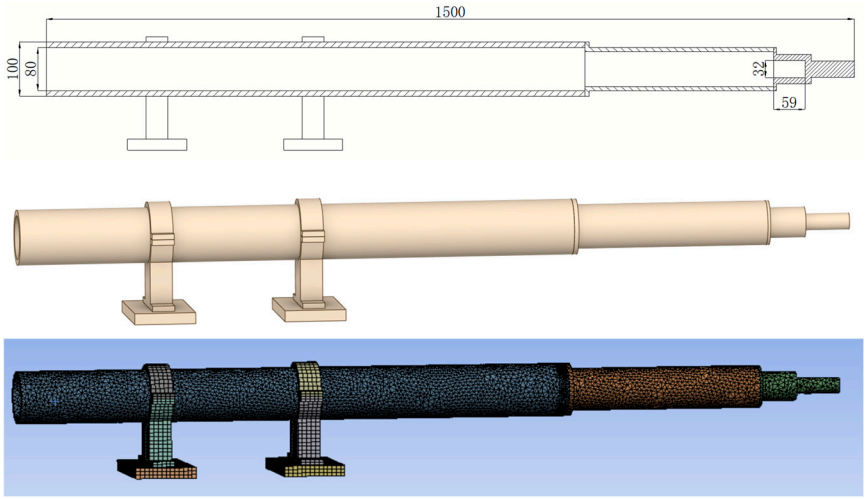


Figure 1. Three-dimensional geometric model, sectional view, and finite element meshing of the slender cantilever actuator.

Table 1. Comparison of predicted and experimentally measured natural frequencies.

Mesh Level	Element Count	Node Count	First Natural Frequency (Hz)	Relative Change (%)
Coarse	8452	25,136	68.37	-
Medium-coarse	15,874	48,231	69.92	2.27
Medium	26,148	79,623	70.51	0.84
Fine	36,186	110,058	70.89	0.54
Extra-fine	48,520	147,634	70.93	0.06

Fixed constraint boundary conditions are applied at the root support end of the cantilever actuator, restricting all translational and rotational degrees of freedom to simulate the actual fixed installation state of the positioning mechanism. It should be noted that as modal analysis evaluates the inherent free-vibration characteristics of the structure, no external dynamic excitation is applied at this stage. The low-order modal parameters of the structure are solved and extracted. Modal characteristics are the core inherent dynamic parameters of precision actuation structures, which directly determine the structural vibration response, dynamic stability, and anti-interference ability under external excitation, providing a basis support for the dynamic optimization and vibration suppression design of precision actuators [33].

For the slender cantilever flexible positioning actuator, ignoring minor structural damping and external time-varying excitations, the discretized undamped free vibration governing equation of the structural system can be expressed as:

$$M\ddot{u}(t) + Ku(t) = 0 \tag{1}$$

Assuming that the structural system produces simple harmonic vibration with a modal form of $u(t) = \phi e^{j\omega t}$, substituting the vibration formula into Equation (1), the generalized eigenvalue equation for structural modal analysis is derived as:

$$(K - \omega^2 M)\phi = 0 \tag{2}$$

where M and K denote the mass matrix and stiffness matrix of the cantilever actuator system, respectively; $u(t)$ represents the structural nodal displacement vector; ω is the structural natural circular frequency; and ϕ corresponds to the structural vibration mode shape vector. Fundamentally, Formulas (1) and (2) establish the theoretical mathematical framework of structural dynamics, serving as the underlying governing equations that the finite element solver discretizes and computes to accurately extract the modal parameters.

The first three dominant mode shapes of the cantilever actuator are illustrated in Figure 2, and the corresponding modal frequency and vibration characteristic parameters are summarized in Table 2. It can be observed that the low-order modes of the slender cantilever actuator are mainly dominated by bending and torsional vibration, which are likely the main contributors to low-frequency micro-positioning errors of the terminal actuator. The first-order Y-axis bending mode and the second-order X-axis torsional mode concentrate the structural vibration energy, which are extremely susceptible to ambient low-frequency excitations and lead to deteriorated positioning stability.

It is particularly noteworthy that the first-order bending mode (70.892 Hz) and the second-order torsional mode (74.978 Hz) are closely spaced in the frequency domain. While the numerical and experimental studies in this work primarily focus on the Y-direction bending response—as the vertical bending displacement is the dominant factor directly deteriorating aiming accuracy—the potential influence of torsional vibrations cannot be neglected. In actual service environments subjected to multi-directional ambient excitations, the close proximity of these natural frequencies may induce bending-torsion coupled

micro-vibrations. Fortunately, the proposed partitioned particle damper adopts a radially symmetric cylindrical configuration. When structural torsional micro-vibrations occur, the internal particle groups will inevitably experience circumferential micro-slip friction and weak collisions against the inner cavity walls. Consequently, the designed particle damping system inherently possesses multi-dimensional energy dissipation capabilities, enabling it to robustly suppress not only vertical bending but also potential torsional interferences.

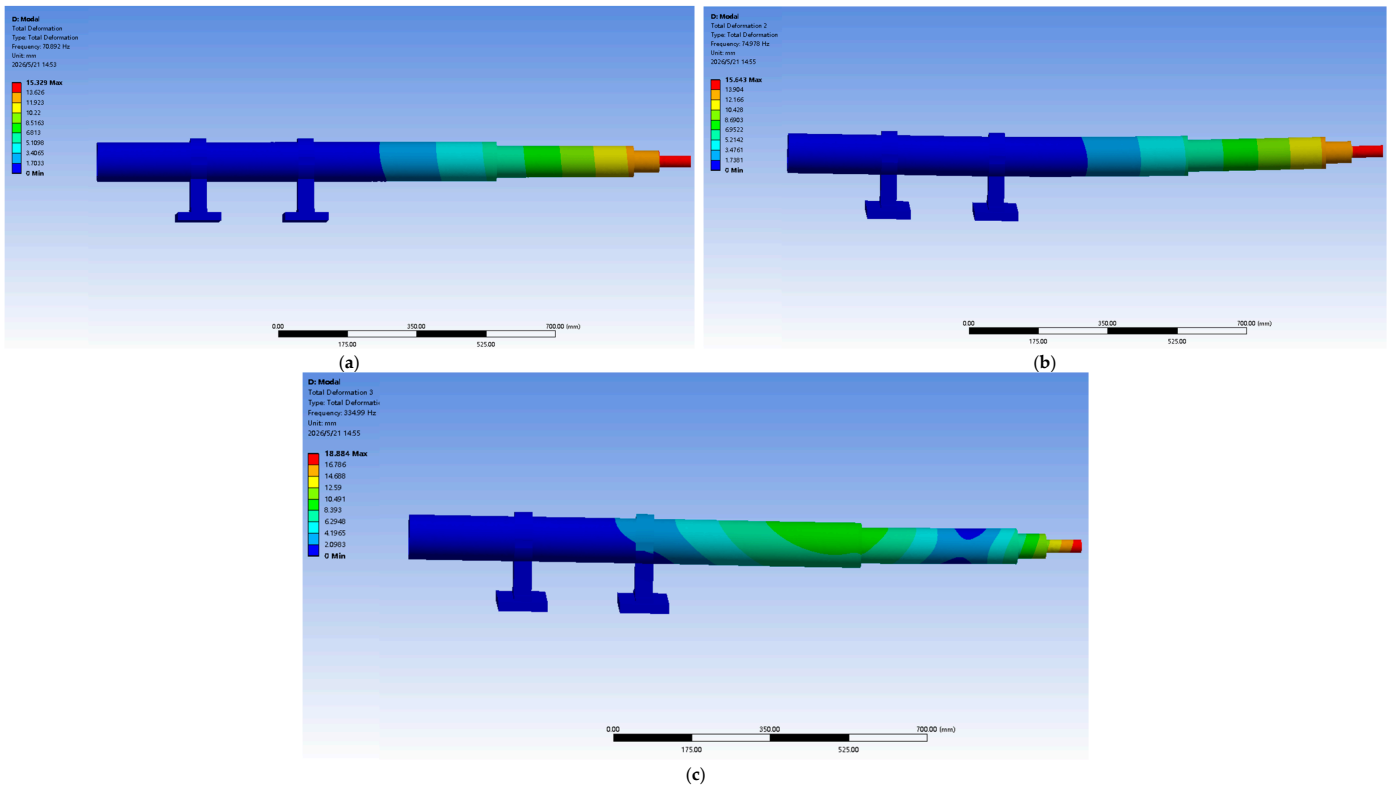


Figure 2. Modal shapes of the slender cantilever precision positioning actuator. (**a**) First-order modal shape; (**b**) Second-order modal shape; (**c**) Third-order modal shape.

Table 2. Low-order modal frequencies and vibration characteristics.

Nth Mode	Modal Frequency/Hz	Mode of Vibration
1	70.892	Y-axis bending
2	74.978	X-axis twisting
3	334.99	Y-axis bending

2.2. Vibration Source Characteristics and Structural Transmission Path Analysis

The terminal positioning accuracy and dynamic stability of slender cantilever precision positioning actuators are jointly determined by structural manufacturing assembly accuracy and external ambient excitation. In practical ultra-precision service scenarios, structural manufacturing errors can be controlled within a small range through high-precision machining and assembly processes. In contrast, ambient low-frequency micro-vibrations transmitted through the foundation and support structure are significant factors inducing terminal micro-displacement errors and stability degradation of precision actuators.

The micro-vibration excitations acting on the cantilever positioning actuator mainly originate from on-site environmental disturbances, including ground traffic vibration, air conditioning system operation, personnel walking, and peripheral mechanical equipment movement. Such environmental micro-excitations are characterized by low frequency

and small amplitude, with an acceleration amplitude ranging from 10^{-5} g to 10^{-3} g (g = 9.8 m/s^2). According to the generic vibration criteria (VC) widely adopted for precision manufacturing and metrology facilities, ambient micro-vibrations induced by ground traffic, building service systems and human activities are typically characterized by dominant spectral energy distributed across the 8–80 Hz band, with pronounced low-frequency components concentrated in the 20–50 Hz range [34]. Therefore, 30 Hz is selected as a representative sub-resonant excitation condition that reflects the typical service environment of the cantilever precision positioning actuator.

Although the excitation amplitude is extremely low, the slender cantilever actuator features low stiffness and weak inherent damping, making it sensitive to low-frequency weak excitations. The ambient micro-vibrations are transmitted along the fixed support base to the cantilever root and further propagated to the terminal execution end, resulting in sustained micro-displacement vibration and prolonged positioning stabilization time, which seriously restricts the ultra-precision positioning performance of the actuator.

The overall vibration transmission path of the slender cantilever positioning actuator is summarized as follows: environmental micro-vibration source → fixed support base → cantilever root constraint interface → cantilever flexible beam structure → terminal positioning end. The terminal end of the cantilever is the final response node of vibration energy and the key area where vibration energy is converted into positioning errors, making it a suitable location for vibration suppression devices.

To intuitively illustrate the dynamic energy flow within the system, a schematic vibration transmission route is explicitly mapped in Figure 3. As depicted, the external environmental excitation is initially inputted through the root base support. Due to the high flexibility of the slender structure, the vibration energy is subsequently transmitted and significantly amplified along the cantilever beam. This amplified dynamic response ultimately reaches the terminal precision actuation mechanism, inducing detrimental micro-vibrations that deteriorate positioning accuracy. By installing the partitioned particle damper at this terminal end, the transmitted vibration energy is effectively captured and dissipated through the intensive frictional micro-slip and inelastic collisions among the internal discrete particles, thereby completely blocking the disruptive energy flow and stabilizing the actuator.

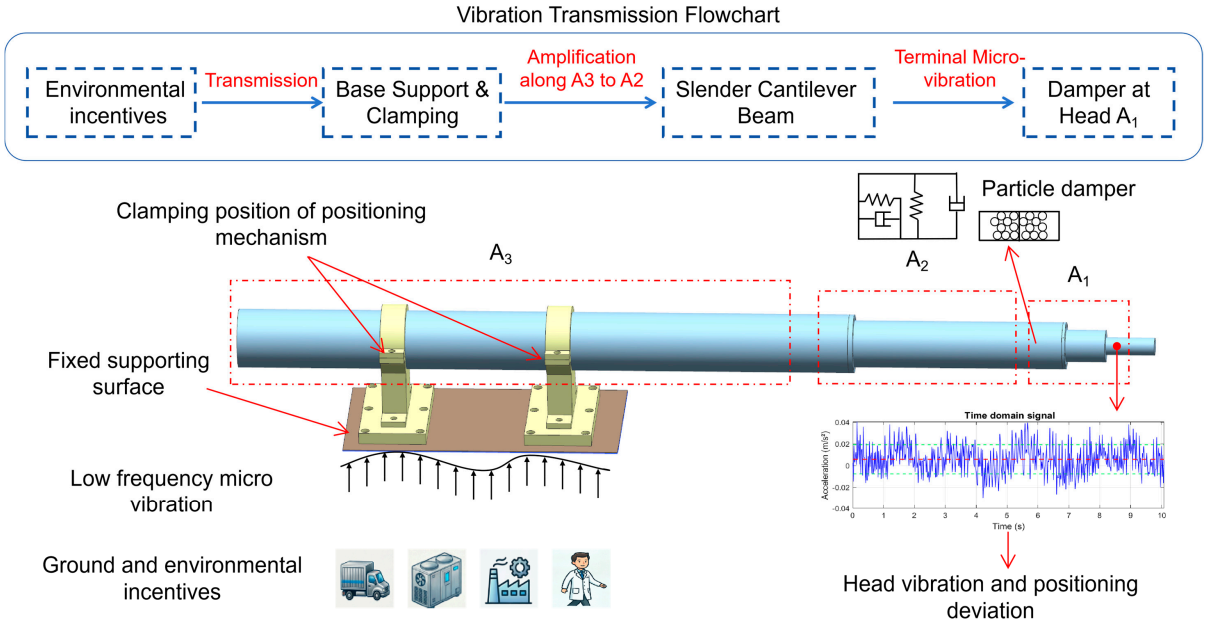


Figure 3. Schematic of environmental vibration excitation, particle damper installation layout, and vibration transmission route.

The theoretical source of this energy dissipation relies on granular mechanics, specifically the intensive momentum exchange, micro-slip friction, and inelastic collisions among particles. While this fundamental passive damping methodology is highly mature and has long been utilized in macro-engineering applications (such as anti-vibration hammers in transmission lines), its direct application to ultra-precision mechanisms requires rigorous scenario-specific adaptations. For the slender cantilever actuator discussed in this work, traditional vibration control methods—such as tuned mass dampers (TMDs) or viscous fluid dampers—are inherently unsuitable due to strict spatial limitations at the terminal cavity, stringent mass payload constraints, and the unacceptable risk of fluid leakage in precision environments. Consequently, the particle damping concept is selected for its exceptional compactness, broad frequency bandwidth, and temperature independence. To specifically adapt to this horizontal low-frequency vibration scenario, a customized partitioned cylindrical structure is proposed. This architectural adaptation effectively prevents the severe agglomeration of particles at the bottom of the cavity induced by gravity, ensuring that the discrete particles maintain optimal mobility and uniform energy dissipation capabilities against complex multi-directional micro-vibrations.

2.3. Frequency-Domain Harmonic Response Characteristic Analysis

Precision positioning actuators inevitably suffer from periodic sinusoidal excitations induced by continuous ambient micro-vibrations during service, which produce frequency-dependent steady-state dynamic responses and further degrade terminal positioning accuracy. To quantitatively characterize the frequency-domain vibration response characteristics of the slender cantilever precision positioning actuator, reveal its vibration energy transmission rules and resonant sensitive frequency bands, and provide a theoretical basis for verifying the broadband low-frequency micro-vibration suppression performance of the subsequent particle damping system, harmonic response analysis based on the modal superposition method is carried out in this work. The governing equation of the forced harmonic vibration system is established as follows:

$$(-\omega^2 M + j\omega C + K)u(\omega) = F(\omega) \tag{3}$$

where C represents the structural damping matrix; $F(\omega)$ is the frequency-domain excitation force vector containing amplitude and frequency characteristics of external micro-excitations; and $u(\omega)$ denotes the complex displacement response vector that contains both vibration amplitude and phase information of structural nodes.

For the 6061 aluminum alloy cantilever actuator, a constant modal damping ratio model was adopted in the finite element harmonic response simulation. This model is selected for its computational efficiency and reliability in characterizing the frequency-independent energy dissipation of the structural system under steady-state harmonic excitation within the low-frequency band of concern. The structural damping ratio was experimentally identified as 0.022 via free-decay tests on the bare cantilever prototype (without particle damper), using the logarithmic decrement method applied to the acceleration decay curve recorded at the terminal positioning end. This baseline damping, primarily arising from material hysteresis and joint friction, ensures that the finite element solver yields finite and physically realistic resonant peak amplitudes, circumventing the theoretically infinite responses that would otherwise occur at resonance.

Combined with the first two-order inherent modal frequencies obtained in the foregoing modal analysis and the actual frequency range of environmental micro-vibrations (1–50 Hz), the harmonic response calculation bandwidth is set to 10–100 Hz to fully cover the dominant low-frequency vibration band and potential resonant frequency domain of the cantilever actuator. The acceleration amplitude frequency response curve at the

terminal positioning end of the slender cantilever precision actuator is solved and plotted in Figure 4.

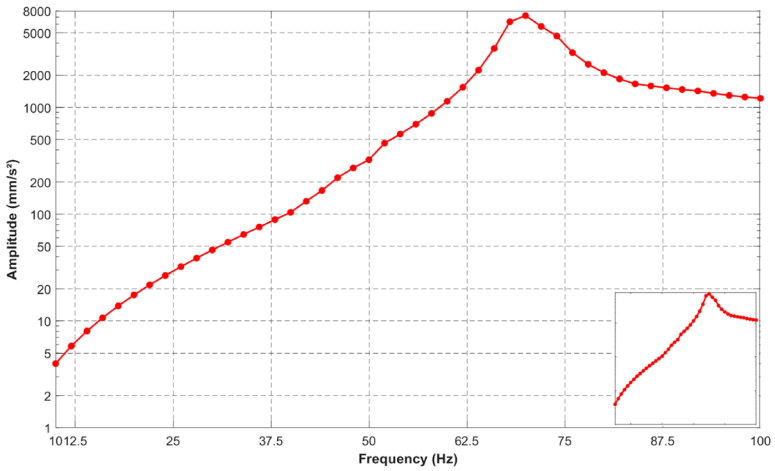


Figure 4. Harmonic response characteristics.

The numerical results indicate that the cantilever actuator exhibits a distinct dominant resonant peak at approximately 70 Hz, which matches well with the first-order bending modal frequency identified in modal analysis. The peak acceleration amplitude reaches up to 7228.5 mm/s^2, demonstrating a significant structural vibration amplification effect occurring at the actuator terminal under undamped conditions, which severely threatens the dynamic stability of the precision positioning system. Within the low-frequency micro-vibration band of 10–60 Hz, the terminal vibration acceleration amplitude presents an approximately logarithmic linear growth trend with the increase in excitation frequency. This low-frequency progressive vibration response is the core factor inducing persistent micro-positioning errors and poor repeatability of the cantilever precision actuator. When the excitation frequency exceeds 70 Hz, the structural response amplitude decreases rapidly and gradually tends to be stable with no obvious vibration amplification phenomenon.

The above frequency-domain response characteristics reveal the low-frequency micro-vibration defect and resonant sensitivity of the slender cantilever precision positioning actuator, verifying the necessity of implementing targeted broadband low-frequency vibration attenuation. Meanwhile, the clarified vibration frequency response rules provide an evaluation benchmark for the subsequent optimization and performance verification of particle damping vibration suppression schemes.

3. Establishment of the Particle Damper Dynamic Model for Precision Actuators

To address the low-frequency micro-vibration problem of slender cantilever precision positioning actuators, a customized particle damper structure is designed in this section. Combined with the operating characteristics of low-amplitude and low-frequency micro-vibrations in precision actuation systems, a refined discrete element numerical model considering micro-scale contact and friction behavior is established. On this basis, the multi-mechanism coupling energy dissipation characteristics of particle damping under micro-vibration conditions are quantitatively decomposed and analyzed. The established theoretical model and numerical framework provide accurate model support for subsequent parametric analysis and vibration suppression performance verification.

It should be emphasized that the microscopic kinematic behaviors of individual particles—including mutual contacts, frictional slips, and inelastic collisions—exhibit significant chaos and randomness under dynamic excitation. To theoretically resolve this

inherent randomness, this section approaches the modeling from a macroscopic statistical perspective based on the principle of equivalent energy dissipation. Rather than tracing the unpredictable trajectory of each discrete particle, the random microscopic interactions are statistically integrated over a complete steady-state vibration cycle to derive a deterministic equivalent macroscopic damping force. Furthermore, the customized partitioned structure physically complements this theoretical treatment. By dividing the global cavity into localized constraints, the spatial degrees of freedom of the particle swarm are strictly limited. This structural restriction effectively suppresses severe random agglomeration and chaotic flow, rendering the collective granular motion more uniform and predictable, thereby ensuring a high degree of consistency between the physical state and the proposed macroscopic theoretical model.

3.1. Structural Design and Layout Optimization of the Particle Damper

Particle damping is a typical nonlinear passive vibration control technology, whose damping performance is highly dependent on external excitation frequency, vibration amplitude, and internal particle motion states. By adjusting structural and physical parameters such as particle diameter, material properties, and filling ratio, targeted damping optimization can be realized for specific vibration environments. In general, vibration suppression strategies for precision actuators can be implemented at the vibration source, transmission path, or terminal response end. In this study, the particle damper is directly installed at the terminal end of the cantilever precision actuator, which enables in-situ dissipation of micro-vibration energy at the maximum vibration response position. This terminal damping layout can effectively suppress multi-source environmental micro-vibrations, demonstrating favorable structural adaptability and vibration robustness for precision positioning systems.

For a fixed particle filling ratio, a reasonably increased damper cavity space can provide sufficient motion margin for particle collision and friction, thereby improving the overall energy dissipation efficiency. Therefore, the dimensional parameters of the damper cavity are constrained by the available installation space at the cantilever actuator terminal. Considering the lightweight integration requirements and convenient parameter debugging of precision actuation equipment, an externally attached modular damper scheme is adopted in this design. The independent damping cavity is fixed to the inner terminal structure of the cantilever actuator through bolting and bonding, which facilitates subsequent disassembly, replacement, and parametric experimental testing.

To increase particle collision frequency and enhance micro-energy dissipation under low-amplitude vibration, the internal cavity is partitioned into multiple independent confined sub-chambers to avoid large-scale particle accumulation and sliding. Accordingly, the designed particle damper adopts a cylindrical aluminum alloy cavity structure with an overall outer diameter of 32 mm and a total length of 55 mm. To avoid large-scale particle accumulation and restrict excessive particle flow, the internal volume is partitioned into ten independent sub-chambers, each featuring an inner diameter of 8 mm and a depth of 26 mm. The damper is fabricated from 6061 aluminum alloy (consistent with the cantilever actuator material) with a uniform wall thickness of 2 mm, ensuring a lightweight structure while providing precise spatial constraints to activate the micro-collision and friction energy dissipation of the particle groups.

3.2. Establishment of Micro-Vibration-Adapted Discrete Element Model

Different from conventional macro-amplitude structural vibration, the low-frequency micro-vibrations of precision cantilever actuators are characterized by ultra-small amplitude, low excitation frequency, and weak structural response. The energy dissipation of

particle damping under such operating conditions mainly relies on weak elastic collision and micro-slip friction between particles and cavity walls, without severe particle jumping or extrusion deformation. To balance numerical calculation accuracy and computational efficiency, this work simplifies the classical discrete element method (DEM) based on the micro-vibration mechanical characteristics, and proposes a refined DEM model suitable for low-frequency micro-vibration scenarios. The core modeling assumptions are summarized as follows:

1. The contact deformation between particles and cavity walls is far smaller than the particle characteristic size, and only elastic contact occurs without plastic deformation or damage;
2. All particle contacts are weak elastic collisions, and contact creep and adhesion effects under micro-amplitude excitation are neglected;
3. The damping cavity is rigidly connected to the cantilever actuator, realizing synchronous micro-vibration without relative sliding displacement;
4. The cavity acceleration amplitude is much lower than gravitational acceleration, and particle agglomeration and large-scale sliding are not considered;
5. Only translational and rotational motion of particles are solved, and additional fluid damping effects are ignored.

Based on the above assumptions, this paper introduces a micro-vibration contact damping correction coefficient λ_m to modify the traditional spring-damper contact model. The particle damping energy transfer process under low-frequency excitation is demonstrated in Figure 5, which intuitively characterizes the micro-scale contact mechanism involving four core mechanical parameters: k_n represents the normal contact stiffness, c_{nm} denotes the micro-vibration normal contact damping, k_t represents the tangential contact stiffness, and c_{tm} denotes the micro-vibration tangential contact damping. Different from conventional macro-vibration contact damping parameters, $\lambda_m \in (0, 1]$ is adopted to characterize the attenuation effect of micro-amplitude excitation on contact energy dissipation. The corrected normal and tangential damping forces are embedded in the contact mechanical model, which improves the model's representation of the actual micro-vibration working conditions.

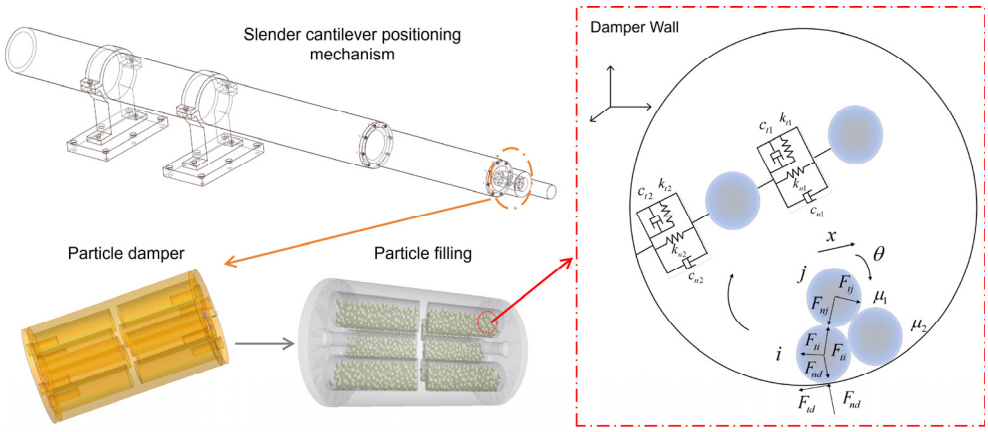


Figure 5. Micro-contact and energy transfer mechanism of particle damping under low-frequency micro-vibration.

At any instantaneous time t, the coupled translational and rotational governing equations of a single particle i are constructed as follows:

$$m_i \ddot{r}_i(t) = m_i g + \sum_j (F_n(t)n(t) + F_t(t)t(t)) - m_i \ddot{r}_c(t) \quad (4)$$

$$I_i\dot{\omega}_i(t) = \sum_j (r(t) \times F_t(t)t(t)) \cdot \eta_m \tag{5}$$

where $\ddot{r}_i(t)$ and $\dot{\omega}_i(t)$ denote the instantaneous translational acceleration and angular acceleration of particle i, respectively; $F_n(t)$ and $F_t(t)$ are the instantaneous normal and tangential contact forces between particle i and particle j (or the cavity wall), respectively. $n(t)$, $t(t)$ and $r(t)$ are the instantaneous unit normal vector, instantaneous unit tangential vector, and instantaneous position vector from the centroid to the contact point at the particle contact point, respectively. $\ddot{r}_c(t)$ is the instantaneous micro-vibration acceleration of the damping cavity, and η_m is the micro-vibration rotational correction coefficient ($\eta_m \in [0.05, 0.2]$) for weak contact motion.

The contact force is decomposed into normal and tangential components. The normal contact adopts a classical linear spring-damper model, which is suitable for weak elastic contact under micro-vibration:

$$F_n(t) = -k_n\delta_n(t) - \lambda_m\eta_n v_n(t) \tag{6}$$

where $\delta_n(t)$ is the normal contact overlap, $v_n(t)$ is the normal relative velocity, k_n is the normal contact stiffness determined by material and geometric parameters, η_n is the normal damping coefficient, and λ_m denotes the micro-vibration damping correction coefficient used for weak-contact damping modification under low-amplitude excitation.

For equal-diameter particles with identical material, the particle–particle normal contact stiffness is derived based on the Hertz contact theory:

$$k_n^{pp} = \frac{2E}{3(1-\nu^2)}\sqrt{2R\delta_n} \tag{7}$$

Considering the spherical–concave cylindrical contact feature between particles and the cylindrical damper cavity, a corrected particle–wall contact stiffness model is adopted to improve calculation accuracy:

$$k_n^{pc} = 2\left(\frac{1-v_p^2}{E_p} + \frac{1-v_c^2}{E_c}\right)^{-1}\sqrt{\frac{R_pR_c}{2R_c - R_p}\delta_n} \tag{8}$$

where v_p, v_c are the Poisson's ratios of particles and damper cavity; E_p, E_c are the corresponding elastic moduli; R_p and R_c represent the particle radius and cavity inner radius, respectively.

The normal damping coefficient is determined by the material recovery coefficient, equivalent contact mass, and normal stiffness, which is universally applicable to micro-impact damping calculation:

$$\eta_n = 2\sqrt{k_n m_{eq}} \cdot \frac{|lne|}{\sqrt{\pi^2 + (lne)^2}} \tag{9}$$

where e is the material recovery coefficient and m_{eq} is the equivalent contact mass of the contact pair.

Under low-frequency micro-vibration conditions, the tangential contact behavior is dominated by micro-slip friction and follows the corrected Coulomb friction criterion. The tangential contact force is constrained by both elastic tangential stiffness and maximum static friction force:

$$F_t(t) = min(k_t\delta_t(t) + \lambda_m\eta_t v_t(t), \mu F_n(t)) \tag{10}$$

where k_t and $\delta_t(t)$ are the tangential contact stiffness and tangential deformation; η_t is the tangential damping coefficient, which takes $\eta_t = \eta_n$ for micro-vibration weak contact; μ is

the sliding friction coefficient of the contact interface. λ_m is the micro-vibration damping correction coefficient matching low-frequency micro-vibration working conditions.

It should be noted that the micro-vibration normal contact damping c_{nm} illustrated in Figure 5 corresponds to the corrected damping term $\lambda_m \eta_n$ in Equation (6), i.e., $c_{nm} = \lambda_m \eta_n$, where η_n is the conventional normal damping coefficient calculated by Equation (9). The same relationship holds for the tangential direction: $c_{tm} = \lambda_m \eta_t$.

The quantitative relationship between tangential and normal contact stiffness is distinguished according to whether the contact materials are consistent, which improves the physical rationality of the model:

$$\begin{cases} k_t/k_n = \frac{1-\nu}{1-\frac{1}{2}\nu}, \text{ Same material} \\ k_t/k_n = \frac{\left(1-\nu_1^2\right)/E_1+\left(1-\nu_2^2\right)/E_2}{(2-\nu_1)/E_1+(2-\nu_2)/E_2} \cdot \frac{1}{2}, \text{ Different material} \end{cases} \tag{11}$$

3.3. Multi-Mechanism Energy Dissipation Mechanism Analysis Under Micro-Vibration

Different from conventional macro-vibration particle damping dominated by collision energy consumption, the low-frequency micro-vibration of slender cantilever precision actuators features weak excitation and small deformation. The system energy dissipation is jointly dominated by micro-slip friction and quasi-static hysteresis extrusion, while micro-collision energy consumption accounts for a relatively small proportion. This section quantitatively establishes the energy dissipation models of three mechanisms to realize full-component decomposition of damping energy consumption.

1. Particles and cavity walls maintain continuous contact under micro-vibration, and relative micro-slip occurs during periodic vibration, producing friction energy dissipation. The friction energy consumption of particle–particle and particle–wall contact pairs is expressed as:

$$\begin{cases} E_{fric1} = \mu_{pp} \cdot F_n^{pp} \cdot \|v_t^{pp}\| \cdot \Delta t, \text{Particle–Particle} \\ E_{fric2} = \mu_{pw} \cdot F_n^{pw} \cdot \|v_t^{pw}\| \cdot \Delta t, \text{Particle–Wall} \end{cases} \tag{12}$$

   where μ_{pp} and μ_{pw} are friction coefficients of particle–particle and particle–wall interfaces; $\|v_t\| \cdot \Delta t$ denotes the tangential micro-slip displacement within a single time step.

2. The particle packing body undergoes periodic compression and release under micro-vibration excitation, forming a force–displacement hysteresis loop. The enclosed area of the hysteresis loop corresponds to the quasi-static extrusion dissipation energy in one vibration cycle:

$$E_{hyst} = 2F_c \cdot \Delta \frac{2}{\alpha+1}_{max} \tag{13}$$

   where F_c is the equivalent Coulomb extrusion force, Δ_{max} is the maximum normal relative deformation of the particle group, and α is the nonlinear exponent characterizing the stiffness hardening behavior of the particle system.

3. Although the excitation amplitude is small, local particles still produce micro-amplitude bouncing and weak collisions. The energy dissipation of single normal collision is calculated by the recovery coefficient method:

$$\begin{cases} E_{\text{coll1}} = \frac{m_i m_j (1-e_{pp}^2)}{2\left(m_i+m_j\right)} \cdot (v_n^{pp})^2, \text{Particle} - \text{Particle} \\ E_{\text{coll2}} = \frac{m_p (1-e_{pw}^2)}{2} \cdot (v_n^{pw})^2, \text{Particle} - \text{Wall} \end{cases} \tag{14}$$

   where e_{pp} and e_{pw} are the recovery coefficients of particle–particle and particle–wall collisions; v_n is the normal relative velocity before collision.

By superposing the three types of energy dissipation components, the total energy dissipation of the particle damping system in the micro-vibration environment can be obtained:

$$E = \sum E_{fric1} + \sum E_{fric2} + \sum E_{hyst} + \sum E_{coll1} + \sum E_{coll2} \quad (15)$$

The established multi-mechanism energy dissipation model can accurately describe the dominant damping characteristics of particle dampers under low-frequency micro-vibration conditions, contributing to addressing the limitation that traditional macroscopic particle damping models are inapplicable to precision actuator micro-vibration scenarios, and providing a theoretical framework for subsequent parametric analysis and damping performance optimization.

4. Determination and Optimization of Key Particle Damper Parameters

The damping performance of particle dampers is highly sensitive to structural and physical parameters, which directly determine the micro-energy dissipation efficiency and low-frequency vibration suppression capability for precision actuation systems. On the basis of the refined micro-vibration coupling dynamic model established in Section 3, this section conducts systematic parametric simulation analysis to clarify the influence mechanism of critical particle parameters on the dynamic damping effect. The optimal parameter configuration is determined to realize targeted low-frequency micro-vibration attenuation of slender cantilever precision positioning actuators, providing a feasible design basis for the engineering application of particle damping in high-precision positioning equipment.

Before proceeding with the systematic parameter optimization, it is essential to clarify the boundary conditions of the design variables. While the number of partitioned chambers significantly influences the spatial distribution and collision frequency of the internal particles, it is treated as a pre-determined structural constant rather than an optimization variable in this section. The specific number of partitions was strategically pre-configured based on the macroscopic geometric boundaries of the actuator's terminal cavity. This structural configuration was designed to strike a necessary physical balance: preventing severe gravity-induced agglomeration through sufficient compartmentalization, while ensuring that each localized chamber retains adequate spatial stroke for the discrete particles to accelerate and execute effective inelastic collisions. Consequently, with the macroscopic structural framework of the partitioned damper firmly established, the subsequent optimization process exclusively focuses on the internal granular state parameters—namely, the particle diameter and the filling rate—to maximize the steady-state energy dissipation efficiency.

In this study, stainless steel particles are selected as the damping medium for the micro-vibration suppression scenario of precision cantilever actuators. Compared with conventional damping materials such as ceramic and tungsten alloy, stainless steel features high density, excellent surface wear resistance, oxidation resistance, and corrosion resistance. Under the same volumetric filling condition, the high-density characteristic provides greater inertial impact force for particle groups, which effectively enhances micro-collision and friction energy dissipation under weak low-frequency excitation. Meanwhile, stainless steel particles possess outstanding mechanical stability and cost economy, making them a suitable damping medium for passive vibration control of slender precision positioning mechanisms.

The stainless steel particles used in this study are 304 austenitic stainless steel, with the following material parameters adopted in all DEM simulations: density of 7.93 g/cm^3, elastic modulus of 196 GPa, and Poisson's ratio of 0.29. The damper cavity is made of 6061 aluminum alloy (density of 2.7 g/cm^3, elastic modulus of 69 GPa, and Poisson's ratio of 0.33), consistent with the cantilever actuator material.

The finite element model of the slender cantilever precision positioning actuator is imported into the discrete element simulation platform. To ensure the accuracy of micro-contact dynamic simulation, the interfacial contact mechanical parameters are calibrated and set as follows: the particle–particle recovery coefficient, static friction coefficient, and rolling friction coefficient are 0.5, 0.48, and 0.05, respectively; the particle–cavity wall recovery coefficient, static friction coefficient, and rolling friction coefficient are 0.45, 0.5, and 0.08, respectively. A particle generation factory is established inside the partitioned damper cavity to achieve uniform particle filling and authentic particle motion state simulation.

Through experimental calibration against free-decay responses of the cantilever prototype under 30 Hz micro-vibration excitation, the micro-vibration correction coefficients are determined as $\lambda_m = 0.35$ for normal/tangential contact damping and $\eta_m = 0.10$ for rotational contact. These values remain constant throughout all parametric simulations.

These values were determined through parameter calibration against experimental free-decay test data of the cantilever prototype under 30 Hz micro-vibration excitation. The correction coefficient λ_m accounts for the reduced energy dissipation efficiency of contact damping under micro-amplitude weak-collision conditions, while η_m characterizes the weak rotational momentum transfer under micro-slip contact. Both parameters were kept constant across all parametric simulations to ensure comparability.

Specifically, the sensitivity analysis reveals that while a 15% variation in λ_m and a 20% variation in η_m induce proportional shifts in the absolute magnitude of total energy dissipation, they do not alter the underlying nonlinear dynamic trends of the system. Furthermore, the structural damping performance exhibits greater sensitivity to λ_m than to η_m. This aligns with the underlying physical mechanisms, as λ_m directly modulates the primary contact damping forces, whereas η_m only governs the secondary rotational momentum transfer. The identified coefficient values ($\lambda_m = 0.35$, $\eta_m = 0.10$) serve as the optimal calibration baseline that most accurately reproduces the experimental free-decay responses. Ultimately, this moderate parameter sensitivity ensures that slight numerical deviations in the correction coefficients do not compromise the validity of the established parametric laws or the conclusions regarding the optimal damping configuration.

To reproduce the actual service environment of precision positioning actuators, real environmental low-frequency micro-vibration is adopted as the excitation input. The model is subjected to continuous sinusoidal excitation along the Y-axis, with a set acceleration amplitude of 0.096 mm/s^2 and a dominant excitation frequency of 30 Hz, which covers the typical low-frequency micro-vibration working band of the cantilever precision positioning system.

4.1. Particle Damping Performance Analysis Under Different Particle Sizes

Particle size is one of the key design parameters affecting the nonlinear energy dissipation characteristics of particle dampers. The particle diameter comprehensively determines the inertial mass of individual particles, the internal contact frequency of the particle group, collision intensity, and overall flow motion state. Especially under ultra-low amplitude micro-vibration conditions, the scaling effect of particle size significantly changes the ratio between surface adhesion force and inertial force, thereby directly dominating the micro-energy dissipation behavior of particle systems. In this section, the damper is installed at the terminal sensitive vibration response area of the cantilever actuator to investigate the vibration suppression performance of different particle sizes under a fixed volumetric filling ratio of 70%. Eight groups of typical particle diameters are selected for comparative simulation, including 0.5 mm, 0.7 mm, 0.8 mm, 1.0 mm, 1.4 mm, 1.5 mm, 1.8 mm, and 2.0 mm. The overall simulation model and particle filling morphology under partial particle size conditions are displayed in Figure 6.

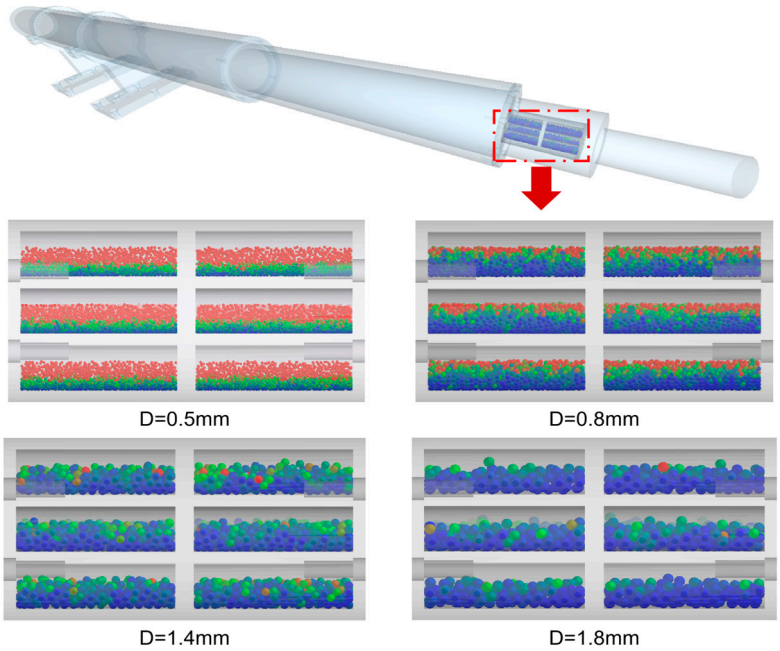


Figure 6. Simulation model and partial particle size filling diagram.

The energy dissipation results of particle dampers with different particle sizes are summarized in Figure 7. The simulation results indicate an obvious nonlinear unimodal correlation between particle size and system energy consumption. Due to the small mass of fine particles, their inertial force is insufficient to overcome the inter-particle friction and geometric interlocking under low-amplitude excitation. This leads to a jamming effect where particles move as a cluster rather than individually, limiting relative sliding and collision, and resulting in insufficient energy dissipation and poor damping performance.

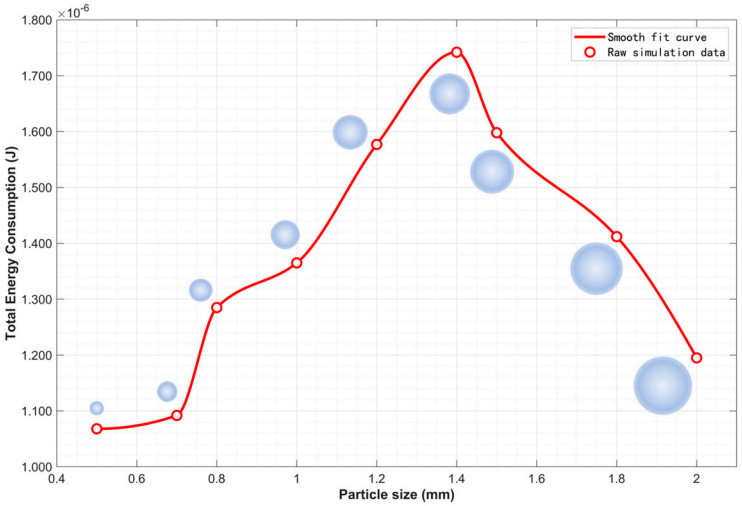


Figure 7. Single-cycle energy dissipation performance of particle dampers with varying particle sizes.

With the gradual increase in particle diameter, the inertial force of individual particles increases significantly, which reduces the adhesion clustering effect. The internal particle collision frequency and micro-slip friction degree are improved, and the overall energy dissipation efficiency of the damper is continuously enhanced. However, when the particle size exceeds the optimal threshold, the total number of particles in the limited cavity decreases sharply, leading to a substantial reduction in cumulative collision times and friction contact area. Although the single-particle collision energy increases, the total

system energy consumption declines. The corresponding single-cycle energy dissipation values for different particle sizes are listed in Table 3.

Table 3. Energy dissipation table of dampers with different particle sizes.

Particle Sizes (mm)	Energy Consumption ($\times 10^{-6}$ J)
0.5	1.068
0.7	1.092
0.8	1.285
1.0	1.365
1.2	1.577
1.4	1.742
1.5	1.598
1.8	1.412
2.0	1.195

It can be concluded that the damping energy consumption increases first and then decreases with the growth of particle size, presenting a typical unimodal nonlinear variation law. There exists an optimal particle size that maximizes the micro-vibration energy dissipation capacity of the damping system. For the slender cantilever precision positioning actuator and partitioned damper configuration proposed in this study, the particle diameter of 1.4 mm achieves the optimal damping performance, with a maximum single-cycle total energy consumption of 1.742×10^{-6} J. This parameter provides the core optimal size basis for the subsequent design and experimental verification of particle dampers for low-frequency micro-vibration suppression of precision actuators.

4.2. Particle Damping Performance Under Different Particle Filling Ratios

The particle filling ratio, defined as the volumetric ratio of particle damping media to the effective damper cavity volume, is a critical structural parameter that governs the particle packing state, internal contact network, and overall damping mass of particle dampers. Variations in filling ratio directly alter the particle collision frequency and micro-slip friction conditions under low-frequency micro-vibration excitation, significantly affecting the passive energy dissipation capacity and vibration suppression performance of precision actuator damping systems. Based on the optimal particle size of 1.4 mm determined in the previous section, a two-stage parametric simulation strategy combining wide-range traversal and local refined optimization is adopted to explore the optimal filling ratio configuration for low-frequency micro-vibration suppression.

4.2.1. Wide-Range Traversal Analysis of Filling Ratio

To clarify the overall variation law of damping performance with filling ratio, four typical filling ratios of 65%, 75%, 85%, and 95% are selected for wide-range simulation traversal. Consistent low-frequency sinusoidal micro-vibration excitation is adopted as the system input to ensure the credibility and comparability of simulation results. The single-cycle energy dissipation values corresponding to different filling ratios are summarized in Table 4.

Table 4. Energy consumption of filling rate wide range search.

Filling Rate	Energy Consumption ($\times 10^{-6}$ J)
65%	1.58
75%	1.67
85%	2.01
95%	2.13

The simulation results indicate that the energy dissipation capacity of the particle damper increases monotonically with the rising filling ratio within the tested wide range. The maximum energy consumption is achieved at the filling ratio of 95%. From the perspective of micro-mechanism evolution, a low filling ratio corresponds to sparse particle distribution and large internal gaps in the cavity, resulting in insufficient particle contact and limited micro-energy dissipation. With the increase in filling ratio, particles gradually transform from a discrete sparse state to a dense packing state. Under weak low-frequency micro-vibration excitation, abundant relative micro-slip and slight local collisions occur between particle groups, which activate the friction and collision energy dissipation mechanisms. Nevertheless, the growth rate of energy dissipation gradually slows down with the continuous increase in filling ratio, presenting an obvious saturation trend, indicating that increasing the filling ratio beyond a certain point yields diminishing returns in terms of damping performance. To capture the optimal filling ratio with the highest damping efficiency, local refined optimization is carried out near the high-efficiency filling interval obtained from wide-range traversal.

4.2.2. Local Refined Optimization of Optimal Filling Ratio

To further pinpoint the optimal filling ratio for low-frequency micro-vibration damping, five refined gradient filling ratios of 90%, 92%, 94%, 96%, and 98% are selected for comparative simulation, with the particle size fixed at 1.4 mm and the excitation conditions kept consistent. The particle distribution morphologies and internal motion energy characteristics under different filling ratios are illustrated in Figure 8. The internal tangential force distribution cloud diagram intuitively reveals the microscopic contact mechanical behavior, spatial contact network evolution, and force transmission path of the particle damping system under varying packing densities.

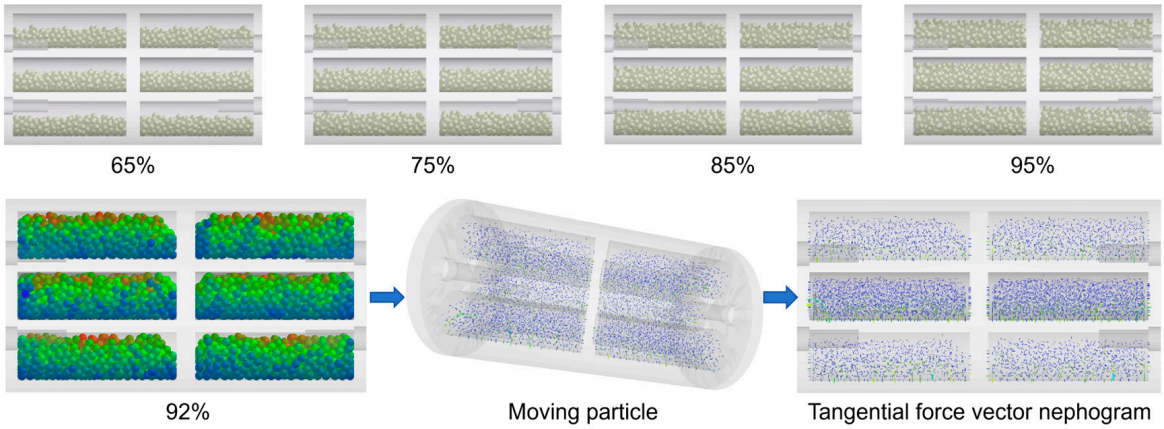


Figure 8. Diagram of different filling rates and particle motion energy.

Combined with the discrete element calculation results of energy dissipation under refined filling ratio gradients presented in Figure 9, the microscopic mechanism by which the filling ratio affects damping performance is further clarified. Within the limited confined volume of the damper cavity, a moderate increase in filling ratio can enrich the particle contact network, improve the frequency of particle–particle and particle–wall micro-collisions and micro-slips, and thus enhance the overall energy dissipation efficiency. However, an excessively high filling ratio will lead to over-dense particle packing, reduce the effective particle motion space, and result in rigid overall particle motion. In this case, the relative micro-slip and collision behaviors are significantly inhibited, which instead weakens the damping energy dissipation capacity.

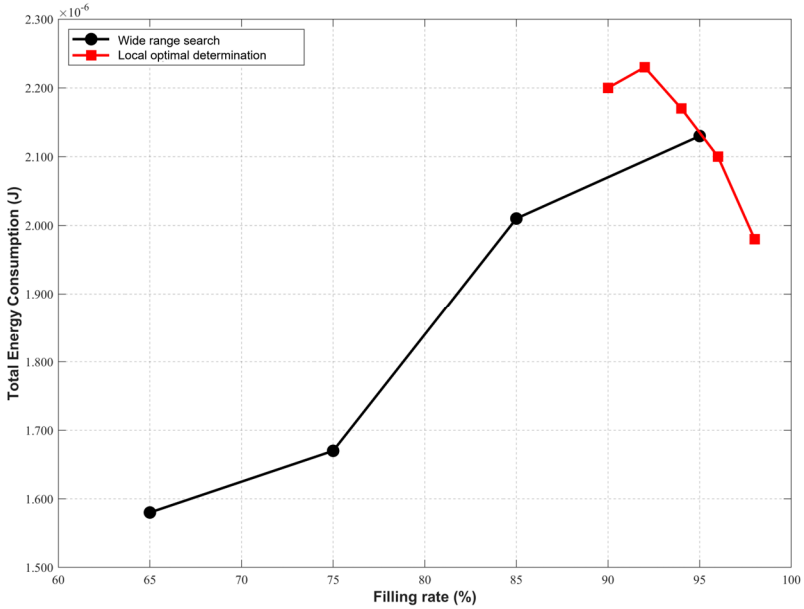


Figure 9. Energy consumption diagram for different filling rates.

The refined simulation results demonstrate that the particle damper achieves the optimal low-frequency micro-vibration energy dissipation performance at a filling ratio of 92%, with a maximum single-cycle energy consumption of 2.23×10^{-6} J. This optimal filling ratio realizes the best balance between particle contact density and effective motion space, maximizing the micro-energy dissipation efficiency of the damping system for precision cantilever actuator micro-vibration suppression.

4.3. Coupling Correlation Analysis of Particle Size and Filling Ratio

The above single-variable analysis clarifies the independent influence mechanism of particle size and filling ratio on the nonlinear energy dissipation characteristics of particle dampers under low-frequency micro-vibration conditions, and obtains the optimal single-parameter intervals. However, in practical engineering applications of precision actuator damping design, the two key parameters are not independent of each other. The particle size determines the basic unit scale of the damping medium, while the filling ratio restricts the packing compactness and effective motion margin of particle groups in the confined cavity. There exists a strong coupling correlation between them, which jointly dominates the overall contact state and energy dissipation efficiency of the particle damping system. Therefore, exploring the coupling matching law of particle size and filling ratio is important for determining an effective damping configuration for slender cantilever precision positioning actuators.

In this section, a multi-parameter coupling simulation test is carried out with consistent model settings and micro-vibration excitation conditions. Five typical particle sizes (0.8 mm, 1.0 mm, 1.4 mm, 1.5 mm, 1.8 mm) and four high-efficiency filling ratios (90%, 92%, 94%, 96%) are selected for cross-group simulation. The energy dissipation performance of particle dampers under various coupling combinations of particle size and filling ratio is comprehensively compared and visualized in Figure 10.

The coupling simulation results verify the existence of a unique optimal parameter matching relationship for the particle damping system targeting low-frequency micro-vibration suppression of precision cantilever actuators. The parameter combination of 1.4 mm particle size and 92% filling ratio achieves the maximum energy dissipation efficiency, which is consistent with the optimal single-parameter results obtained from independent variable analysis. Reasonable coupling matching of particle size and filling ratio

can configure favorable spatial motion conditions for particle groups, promote micro-slip friction and inelastic collision energy dissipation behaviors, and avoid insufficient contact caused by sparse packing or rigid motion caused by over-dense packing.

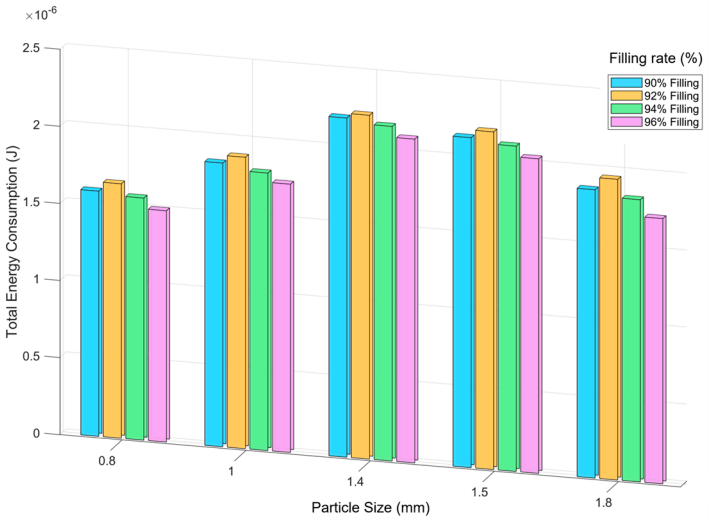


Figure 10. Optimal solution for energy consumption of particle damper.

This study confirms that customized parameter matching is required for particle dampers applied to precision actuator micro-vibration suppression. Simply optimizing a single parameter cannot maximize the damping performance. The established coupling parameter optimization strategy offers a design approach for particle damping configuration of slender cantilever precision positioning mechanisms, which contributes to the practicability and engineering applicability of passive micro-vibration suppression technology for high-precision actuation systems.

5. Experimental Verification of Vibration Suppression Performance for Slender Cantilever Precision Positioning Mechanism

Numerical simulation and parametric analysis in the previous sections have clarified the independent and coupling influence laws of particle size and filling ratio on the micro-vibration energy dissipation performance of particle dampers, and preliminarily determined the optimal parameter matching scheme. To further validate the validity of the established dynamic model and the effectiveness of the optimized particle damping vibration suppression method, experimental tests are carried out on the slender cantilever precision positioning mechanism in this section. By comparing the vibration response characteristics of the actuator before and after damping treatment under low-frequency micro-vibration excitation, the actual vibration reduction performance of the particle damper is quantitatively evaluated, which provides reliable experimental support for the engineering application of particle damping technology in high-precision positioning actuators.

The experimental prototype adopts a slender cantilever structure consistent with the numerical model, with overall dimensions of 1500 × 100 × 150 mm, a wall thickness of 10 mm, and 6061 aluminum alloy as the structural material. The low-frequency micro-vibration excitation environment required for the test is realized by an SZ/ZD-LD six-degree-of-freedom electromagnetic vibration test bench (Suzhou Shuozhou Technology Co., Ltd., Suzhou, China). The vibration bench supports a frequency range of 1–600 Hz and an amplitude adjustment range of 0–5 mm, which can reproduce the low-frequency micro-excitation environment of precision actuators in actual service scenarios.

In this test, a 1A731E three-axis piezoelectric vibration sensor (Jiangsu Donghua Testing Technology Co., Ltd., Jingjiang, China) is deployed to collect the terminal vibra-

tion response of the cantilever positioning mechanism. The sensor exhibits favorable low-frequency measurement performance, with an axial sensitivity of 10 mV/(m·s^{-2}) (23 ± 5 °C), a wide frequency response range of 0.5–5000 Hz, and a high resolution of 0.0002 g. The lightweight sensor structure (180 g) effectively avoids additional structural interference on the precision cantilever mechanism, to ensure reliable micro-vibration test data.

In the experiment, sinusoidal low-frequency micro-vibration excitation is applied along the dominant Y-direction of the cantilever actuator. The excitation acceleration amplitude is set to 35 mm/s^2 with a vibration frequency of 30 Hz, which matches the simulation excitation conditions. To ensure the reliability and reproducibility of the measurements, each experimental condition was independently repeated five times (N = 5) under identical laboratory conditions. The structure was fully rested between consecutive trials to eliminate any residual thermal or dynamic effects.

To guarantee the accuracy of the base excitation and address the absence of a real-time closed-loop control on the shaker, a rigorous pre-test calibration procedure was conducted prior to the formal experiments. The functional relationship between the input drive voltage of the controller and the resulting base acceleration was carefully mapped and verified using a reference accelerometer. During the actual tests, the shaker was operated under these pre-calibrated settings, ensuring that a consistent base excitation amplitude of 35 mm/s^2 was accurately delivered to the cantilever structure.

The vibration response characteristics of the cantilever terminal are evaluated by the root mean square (RMS) value of acceleration, which reflects the steady-state vibration level and positioning stability of the precision actuator. The overall experimental layout, fixed support mode, and sensor measuring point arrangement are illustrated in Figure 11. The vibration transmission path of the test system follows: vibration test bench → fixed base (A3) → cantilever extension section (A2) → terminal positioning end (A1).

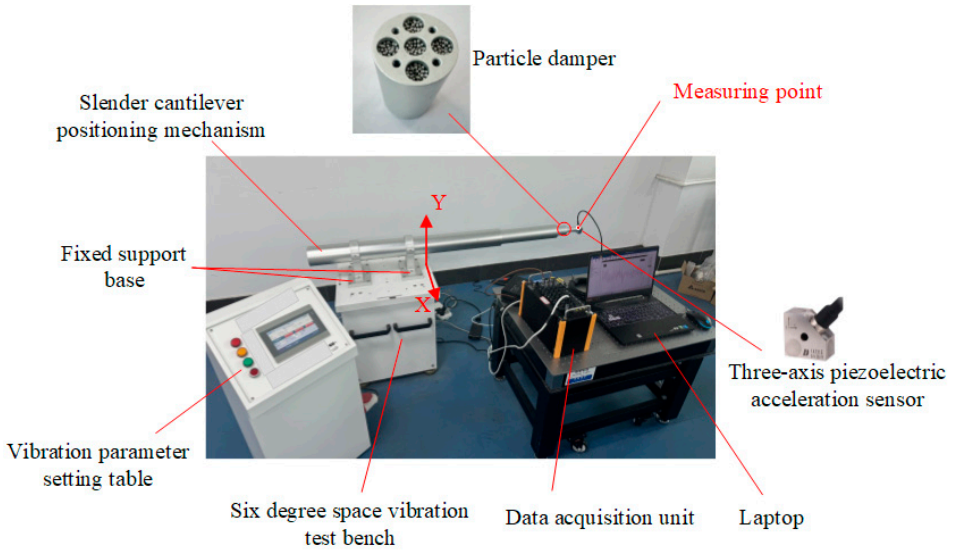


Figure 11. Integral fixed orientation and measuring points.

5.1. Experimental Optimization and Verification of Optimal Particle Size

To quantitatively explore the influence of particle size on the low-frequency micro-vibration suppression performance of particle dampers and verify the optimal particle size obtained from numerical simulation, single-factor controlled variable experiments are conducted in this section. The cantilever prototype is rigidly fixed on the vibration test bench to ensure consistent excitation input. A total of eight groups of stainless steel particles with typical diameters (0.5 mm, 0.7 mm, 0.8 mm, 1.0 mm, 1.4 mm, 1.5 mm, 1.8 mm,

and 2.0 mm) are selected for comparative damping tests. The physical morphology of stainless steel particles with different sizes is displayed in Figure 12.

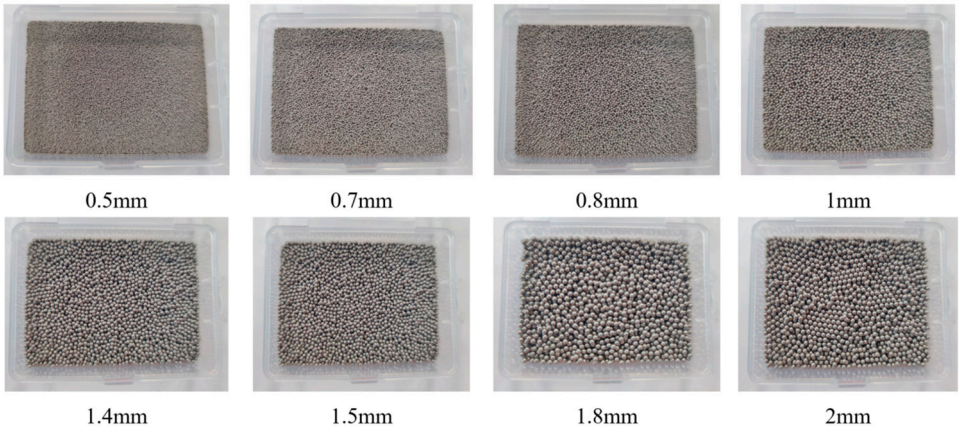


Figure 12. Particle diagram of stainless steel with different particle sizes.

To ensure the comparability of experimental results, the particle filling ratio is fixed at 70% for all test groups. The unified particle filling mode and damper installation position at the cantilever terminal sensitive vibration region are shown in Figure 13. The terminal acceleration RMS values (presented as mean ± standard deviation) and the corresponding vibration damping rates under different particle size conditions are summarized in Table 5.

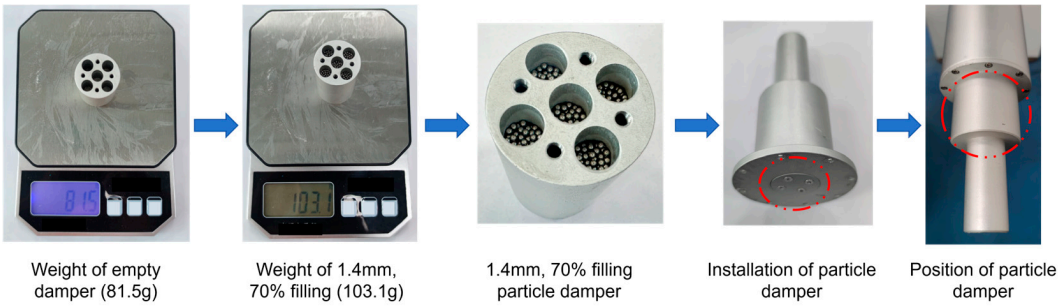


Figure 13. Particle filling mode and damper installation position.

Table 5. RMS value of acceleration (Mean ± SD) with or without damping.

Working Condition	Y-Direction RMS/(mm/s^2)	Damping Results
No damper	45.64 ± 0.36	—
Particle size (0.5 mm)	33.45 ± 0.28	26.71%
Particle size (0.7 mm)	31.62 ± 0.31	30.72%
Particle size (0.8 mm)	30.27 ± 0.24	33.68%
Particle size (1.0 mm)	27.01 ± 0.22	40.82%
Particle size (1.4 mm)	21.92 ± 0.16	51.97%
Particle size (1.5 mm)	22.68 ± 0.21	50.31%
Particle size (1.8 mm)	26.35 ± 0.23	42.27%
Particle size (2.0 mm)	31.36 ± 0.26	31.29%

The experimental results indicate that the particle size exhibits a significant unimodal nonlinear effect on the damping performance of precision cantilever actuators. With the particle size increasing from 0.5 mm to 1.4 mm, the micro-collision and micro-slip friction behaviors inside the damper are fully activated, the system energy dissipation capacity is continuously improved, and the terminal micro-vibration suppression effect is gradually optimized. The optimal damping performance is achieved at the particle size of 1.4 mm,

with a maximum vibration attenuation rate of 51.97% in the main vibration direction, which suppresses the low-frequency positioning vibration of the precision actuator.

When the particle size exceeds 1.4 mm, the limited cavity volume leads to a sharp reduction in the number of particles and contact pairs, resulting in decreased friction collision efficiency and weakened overall damping performance. The vibration attenuation rate decreases significantly with the further increase in particle size. The comparison between experimental damping characteristics and numerical simulation energy consumption results is presented in Figure 14, where the left axis represents the single-cycle energy loss and the right axis denotes the actual vibration damping rate.

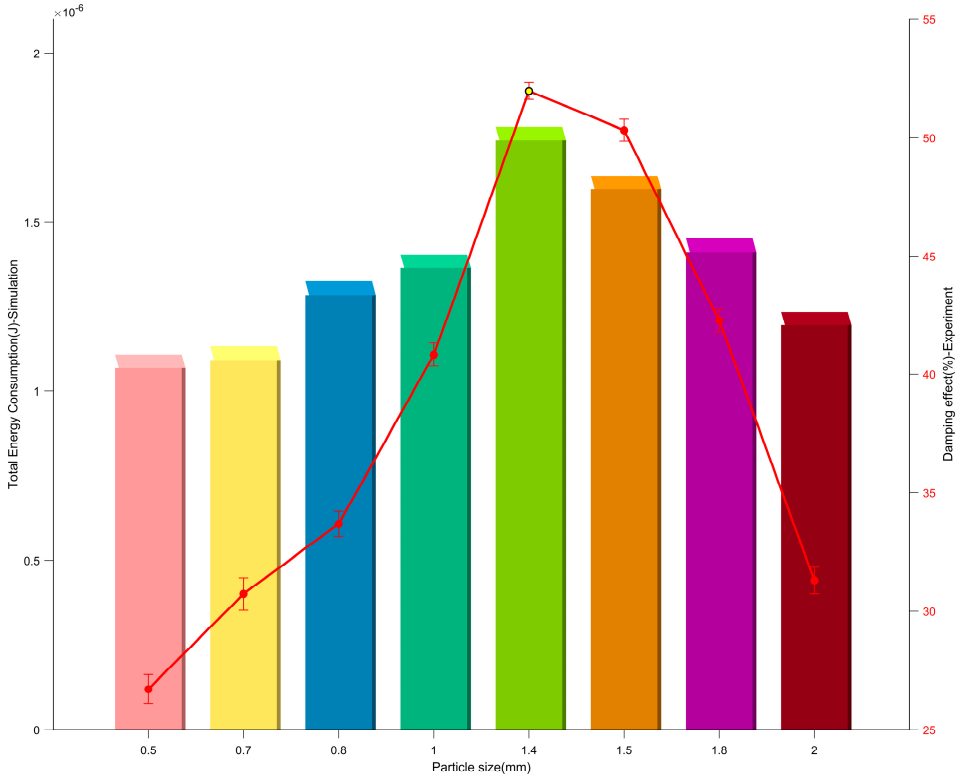


Figure 14. Figure of experimental and simulation data.

The experimental vibration damping curve exhibits a trend highly consistent with the simulated energy consumption curve, thereby substantiating the validity of the proposed dynamic model. To quantitatively assess this agreement, the Pearson correlation coefficient r between the simulated total energy consumption and the experimental damping effect was calculated. The analysis yields $r = 0.981$, indicating a highly significant positive correlation. Consequently, both simulation and experimental results confirm that a particle size of 1.4 mm is optimal for the designed partitioned particle damper, effectively enabling low-frequency micro-vibration suppression in slender cantilever precision positioning mechanisms.

5.2. Experimental Optimization and Verification of Optimal Particle Filling Ratio

Based on the determined optimal particle size of 1.4 mm, this section further explores the influence of particle filling ratio on the low-frequency micro-vibration suppression performance of particle dampers through controlled variable experiments. To guarantee experimental consistency, all test conditions and sinusoidal micro-vibration excitation parameters remain identical to the previous particle size tests. Five refined filling ratio gradients of 90%, 92%, 94%, 96%, and 98% are selected for comparative damping experiments, and the terminal acceleration RMS values (presented as mean ± standard deviation) of the

cantilever actuator under different filling ratios are statistically analyzed to quantify the damping performance variation, as listed in Table 6.

Table 6. RMS value of acceleration (Mean ± SD) with or without damping.

Working Condition	Y-Direction RMS/(mm/s^2)	Damping Results
No damper	44.83 ± 0.34	—
Filling rate (90%)	17.15 ± 0.14	61.74%
Filling rate (92%)	16.48 ± 0.07	63.24%
Filling rate (94%)	17.55 ± 0.15	60.85%
Filling rate (96%)	18.60 ± 0.17	58.51%
Filling rate (98%)	20.46 ± 0.19	54.36%

The experimental results reveal a distinct nonlinear variation law between filling ratio and damping performance. Among all tested groups, the particle damper with a 92% filling ratio exhibits the optimal low-frequency micro-vibration suppression capability, achieving a maximum vibration damping rate of 63.24% in the dominant Y-direction. This phenomenon is attributed to the optimal matching between particle packing density and effective motion space under this filling ratio, which activates micro-slip friction and weak collision energy dissipation of particle groups. In contrast, insufficient filling leads to sparse particle distribution and inadequate contact energy dissipation, while excessive filling causes over-compaction of particle groups, restricts relative microscopic motion, and significantly weakens the damping effect.

The comprehensive comparison of numerical simulation energy dissipation predictions and experimental damping results under different filling ratios is illustrated in Figure 15, where the simulated energy dissipation values and measured vibration reduction efficiencies present highly consistent variation trends and identical optimal parameter positions. Quantitative analysis yields a Pearson correlation coefficient of $r = 0.998$ between the simulated and experimental datasets. The good quantitative agreement between simulation and experimental data further supports the validity of the micro-vibration damping mechanism model and the rationality of the filling ratio optimization strategy.

5.3. Coupling Parameter Verification and Optimal Damping Configuration Determination

The vibration suppression performance of particle dampers is determined by the coupled interaction of multiple structural parameters, rather than the independent action of a single variable. The above single-factor tests have clarified the optimal individual values of particle size and filling ratio. To further explore the multi-parameter coupling mechanism and obtain the best-performing damping configuration within the tested parameter space for precision cantilever actuators, cross-coupling experimental tests are carried out in this section. Five typical particle sizes (0.8 mm, 1.0 mm, 1.4 mm, 1.5 mm, 1.8 mm) and four high-efficiency filling ratios (90%, 92%, 94%, 96%) are selected for combined parameter testing under consistent micro-vibration excitation conditions.

To quantitatively compare the experimental damping performance with the numerical DEM predictions in the same physical dimension (J), the experimentally measured terminal acceleration was converted into the equivalent energy consumption per cycle. Under the 30 Hz steady-state harmonic excitation, the dynamic response of the slender cantilever actuator is dominated by a single frequency. Consequently, the steady-state displacement amplitude X can be derived from the measured acceleration amplitude a and the excitation angular frequency ω using the relationship $X = a/w^2$. Based on the principles of structural dynamics, the equivalent energy dissipated by the particle damper within a single vibration cycle, E_{exq}, was indirectly evaluated through the structural equivalent modal parameters and the measured amplitude reduction. This experimentally derived energy consumption

provides a unified metric for evaluating the cross-coupling effects of particle size and filling ratio, as illustrated in Figure 16.

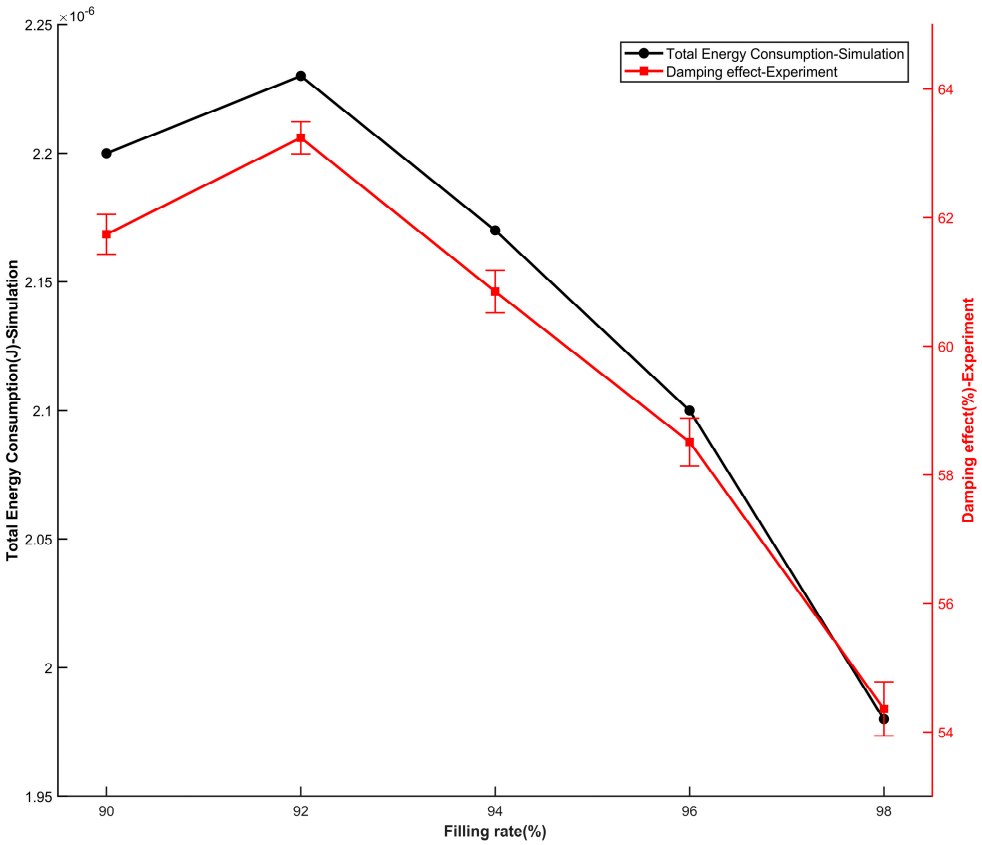


Figure 15. Comparison between experiment and simulation under different filling rates.

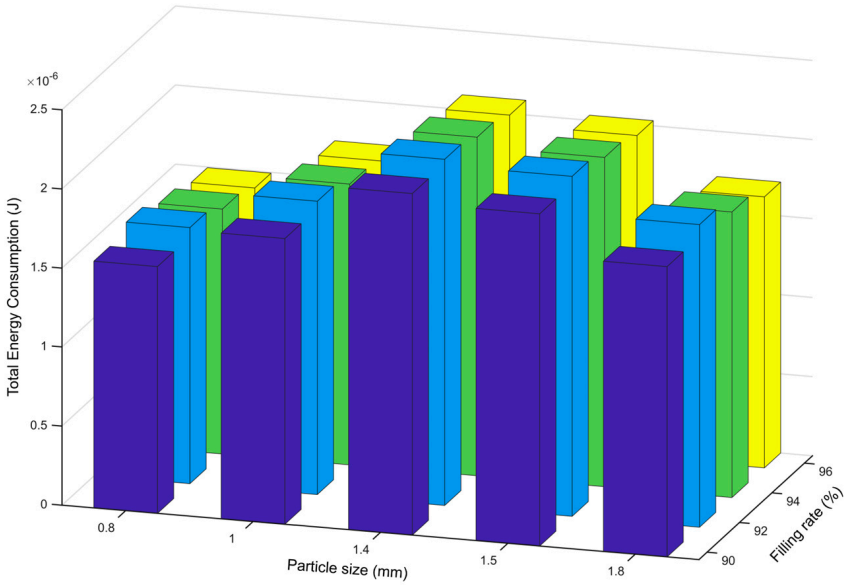


Figure 16. Experimentally derived energy consumption under different particle size and filling ratio combinations.

Furthermore, a quantitative comparison reveals that the relative error between the simulated energy consumption and the experimentally derived equivalent energy consumption under the optimal configuration (1.4 mm, 92%) is only 1.87%. This small quantitative discrepancy directly verifies the prediction accuracy of the established discrete element model.

The test results demonstrate that the coupling combination of 1.4 mm particle size and 92% filling ratio achieves the maximum vibration attenuation rate of 63.24%, which performed better than other tested combinations. When the filling ratio exceeds the optimal threshold, excessive particle compaction limits the relative micro-motion of particle groups, resulting in a sharp decline in damping efficiency. When the particle size deviates from the optimal value, the dynamic balance between particle contact quantity and collision friction efficiency is broken, which reduces the effectiveness of the micro-energy dissipation advantage of the damping system.

To ensure full reproducibility and facilitate practical engineering evaluation of the proposed damping system, the detailed physical parameters of the optimal particle damper configuration (1.4 mm particle diameter, 92% filling ratio) are comprehensively summarized in Table 7.

Table 7. Physical specifications of the optimal particle damper assembly.

Parameter Category	Specific Parameter	Value
Mass Distribution	Empty Damper Cavity Mass	81.5 g
	Mass of Filled Particles (92% ratio)	28.6 g
	Total Added Mass to Actuator	110.1 g
Discrete Properties	Particle Material	304 Stainless Steel
	Particle Diameter	1.4 mm
	Total Particle Number	~2560

Combining single-factor optimization laws, multi-parameter coupling test results, and repeated stability verification experiments, the most effective discrete parameter configuration of the particle damper tailored for the slender cantilever precision positioning mechanism is finally determined: a stainless steel particle size of 1.4 mm and a filling ratio of 92%. This customized matching scheme realizes the optimal balance of particle contact density and motion margin, enhancing the low-frequency micro-vibration energy dissipation efficiency of the damping system.

To rigorously distinguish the energy dissipation capability of the particle damper from the passive mass-loading effect, a control experiment utilizing an "empty-damper" configuration was conducted. In this control case, a solid aluminum slug with a mass equivalent to the total mass of the particles in the optimized configuration (1.4 mm particle size, 92% filling ratio) was rigidly fixed inside the damper cavity. This setup ensured that the total mass added to the cantilever tip was identical to that of the particle-filled case, thereby isolating the damping contribution derived solely from the added weight. The vibration suppression performance of the empty-damper case was then compared with the original structure (no damper) and the optimized particle damper under identical excitation conditions (30 Hz sinusoidal vibration).

The quantitative comparison of the Root Mean Square (RMS) acceleration responses is summarized in Table 8. The experimental results indicate that the empty-damper configuration achieved a damping rate of only 8.0%, reducing the RMS acceleration from 44.83 mm/s^2 to 41.25 mm/s^2. This marginal reduction is primarily attributed to the mass-loading effect, which slightly shifts the system's natural frequency away from the excitation frequency. In stark contrast, the particle-filled damper demonstrated a significantly superior performance, achieving a damping rate of 63.24% with an RMS acceleration of 16.48 mm/s^2.

The substantial discrepancy between the two configurations—specifically the additional 55.24% reduction in vibration amplitude provided by the particle damper—confirms that the primary suppression mechanism is not merely the added mass. Instead, the results validate that the enhanced energy dissipation is driven by the nonlinear interactions of

the particles, including inter-particle collisions and friction against the cavity walls. This comparative analysis conclusively separates the damping effect from the mass-loading effect, verifying the efficiency of the proposed particle damping mechanism.

Table 8. Comparison of vibration damping performance for different configurations.

Configuration	RMS Acceleration (mm/s^2)	Damping Rate (%)
No damper	44.83	—
Empty Damper (Mass Loading)	41.25	8.0%
Particle Damper (Optimized)	16.48	63.24%

To further quantitatively evaluate the transient vibration suppression effect of the optimal damping configuration, time-domain vibration response tests are conducted under 30 Hz fixed-frequency sinusoidal excitation consistent with actual environmental micro-vibration characteristics. The time-domain acceleration response curves of the cantilever terminal before and after damper installation are compared in Figure 17. It can be intuitively observed that the optimal particle damper achieves significant suppression of structural micro-vibration: the high-frequency violent oscillation components are attenuated, and the terminal acceleration response is stably controlled within ± 30 mm/s^2 in most working cycles. Meanwhile, the peak acceleration of the precision actuator is reduced by 67.5%.

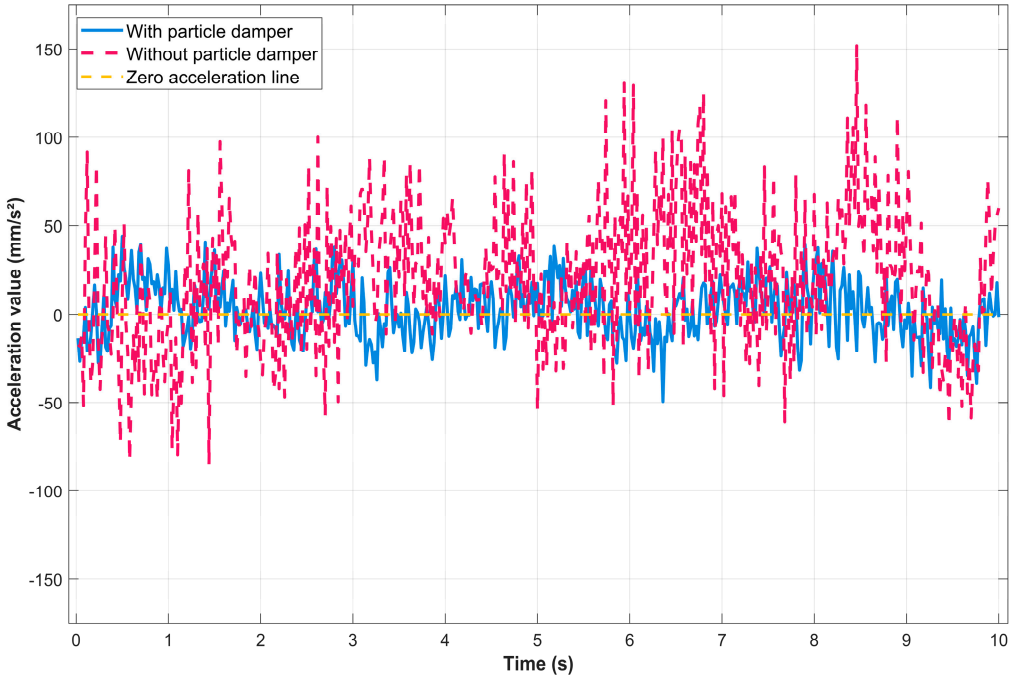


Figure 17. Time domain diagram of measuring points before and after damper installation.

The above time-domain test results confirm the favorable passive damping performance of the optimized particle damper. Through efficient micro-collision and micro-slip friction energy dissipation, the designed damper significantly attenuates the transient dynamic response of the slender cantilever precision positioning mechanism, contributing to the dynamic stability and positioning accuracy of the precision actuation system under low-frequency micro-vibration interference.

5.4. Broadband Sweep Frequency Response Analysis Under Optimal Damping Parameters

In actual service scenarios, precision positioning actuators are usually subjected to broadband variable-frequency micro-vibration interference, rather than single-frequency

excitation. To verify the broadband vibration suppression adaptability of the optimally configured particle damper, this section conducts sweep frequency response tests within a typical low-frequency vibration band of precision equipment. A continuous sinusoidal sweep excitation ranging from 10 Hz to 500 Hz was applied to the cantilever mechanism via the vibration test bench. To ensure the complete capture of the steady-state dynamic response and eliminate transient errors, a linear sweep rate of 1 Hz/s was configured. The excitation amplitude was maintained at a constant acceleration of 35 mm/s^2 across the entire broad band. During data acquisition, the spectral signals were processed with a frequency resolution of 0.5 Hz, and a linear averaging method (5 continuous spectral averages) with a Hanning window was utilized to suppress random environmental noise. Furthermore, to verify the repeatability of the dynamic testing, the full-band sweep procedure was independently repeated three times, and the highly consistent averaged frequency response curves were extracted to systematically analyze the wideband vibration reduction characteristics of the damper.

The broadband sweep frequency response results are presented in Figure 18. The test results indicate that the optimized particle damper exhibits stable vibration suppression performance across the full frequency band of 10–100 Hz, achieving broadband micro-vibration attenuation for precision cantilever actuators. With the increase in excitation frequency, the damping efficiency presents a typical nonlinear variation trend of first increasing and then decreasing.

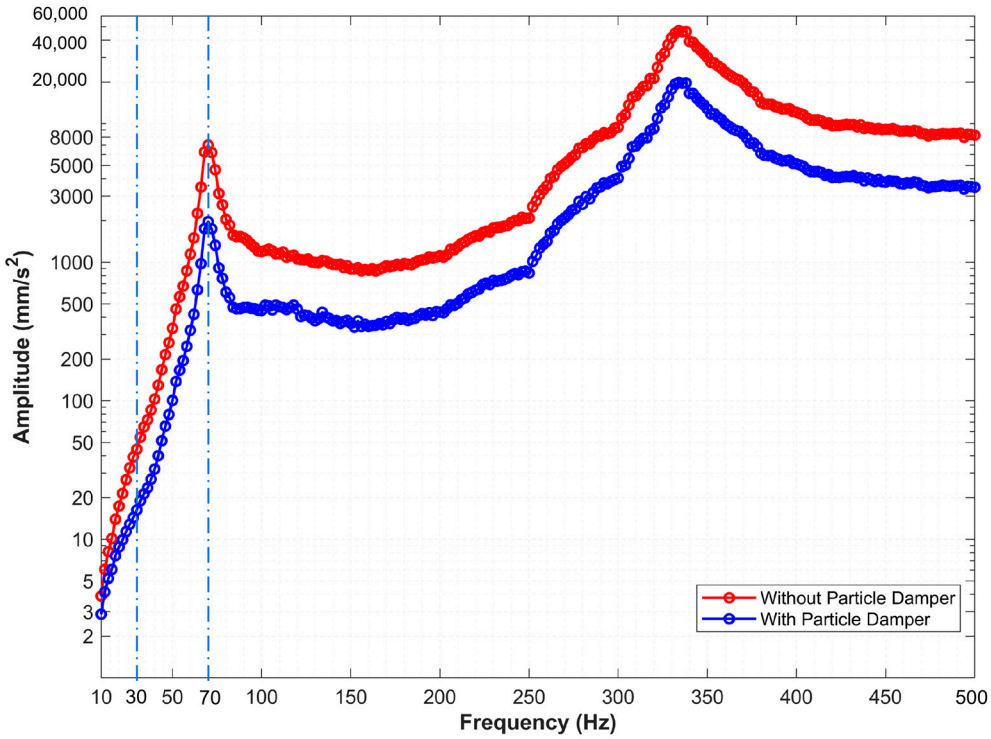


Figure 18. Broadband sweep response diagram under optimal damping parameters.

The maximum damping performance is achieved at the sweep frequency of 70 Hz, which corresponds to the first-order natural frequency of the slender cantilever positioning mechanism. Notably, this experimentally measured resonant frequency closely matches the first-order natural frequency (70.892 Hz) predicted by the numerical modal analysis, which strictly validates the high modeling accuracy of the theoretical eigenvalue equations (Equations (1) and (2)) established in Section 2.1.

At this resonant frequency, the damping loss factor is 45.5% higher than that at 10 Hz, and the structural vibration amplitude attenuation rate reaches a peak value of

72%. Under resonant excitation, the particle group produces synchronous strong resonant response, which significantly increases the relative motion amplitude between particles and cavity walls. The frequency and intensity of micro-collision, friction and extrusion behaviors are stimulated, thereby maximizing the energy dissipation efficiency of the particle damping system. The observed broadband and resonance suppression performance further demonstrates the engineering applicability of the optimized particle damper for dynamic performance improvement of precision positioning actuators.

Remarkably, the vibration response curve with the particle damper remains consistently lower than the undamped curve across the entire 10–500 Hz bandwidth. The damper not only suppresses the primary low-frequency resonance but also effectively attenuates the structural response at the third-order high-frequency mode. No abnormal vibration amplification or unexpected higher-harmonic peaks are generated outside the 10–100 Hz range. These results firmly confirm that the discrete nonlinear impact energy generated under micro-vibration excitation is extremely weak and does not transfer harmful impulsive energy to higher-order structural modes. Consequently, the optimized particle damper exhibits excellent broadband stability and safety, proving its applicability for precision actuation systems without inducing secondary high-frequency disturbances.

It should be noted that particle damping is inherently nonlinear, and its performance is theoretically dependent on excitation frequency and amplitude. To verify the generality of the identified optimal parameters (1.4 mm, 92%), additional comparative analyses were conducted at representative frequencies including 20 Hz, 50 Hz, and 70 Hz (resonance). The results show that although the absolute damping efficiency varies with excitation frequency, the relative ranking of different parameter combinations remains consistent across the 10–100 Hz band. The 1.4 mm + 92% configuration consistently delivers superior or near-optimal damping performance, indicating that the optimal matching is primarily governed by the geometric packing and contact network characteristics within the confined cavity, which are relatively insensitive to moderate frequency variations.

Regarding amplitude dependence, within the micro-vibration acceleration range considered in this study (~0.1 mm/s^2), the particle motion is dominated by micro-slip friction and quasi-static hysteresis rather than large-amplitude bouncing. This friction-dominated regime exhibits milder amplitude sensitivity compared with the collision-dominated regime under strong excitation. The high filling ratio of 92% is particularly adapted to such weak-excitation conditions by providing abundant contact interfaces for frictional energy dissipation.

To quantitatively validate the improvement in the positioning accuracy of the precision actuator, the measured acceleration responses are mathematically converted into equivalent dynamic displacement amplitudes, serving as a direct metric for terminal positioning errors. Under steady-state harmonic excitation, the dynamic displacement amplitude D is derived via the kinematic relationship $D = a/(2\pi f)^2$, where a denotes the acceleration amplitude and f is the excitation frequency.

Based on this conversion, the inherent dynamic positioning error of the undamped cantilever reaches approximately 1.26 μm under 30 Hz non-resonant excitation, and is severely amplified to 36.24 μm at the 70 Hz first-order resonance. These persistent micro-scale vibrational displacements inherently deteriorate the aiming accuracy and operational stability of the precision actuation system. Following the implementation of the optimally configured particle damper (1.4 mm particle size, 92% filling ratio), the positioning error under 30 Hz excitation is effectively suppressed to just 0.46 μm. More significantly, at the critical resonant frequency, the maximum dynamic displacement is dramatically attenuated from 36.24 μm to 10.15 μm, corresponding to a peak vibration reduction rate of 72.0%. Ultimately, this quantitative reduction in dynamic displacement errors robustly substantiates

the capability of the proposed passive particle damping methodology to achieve effective low-frequency micro-vibration attenuation, thereby fundamentally enhancing the terminal positioning accuracy and dynamic stability of slender cantilever precision actuators.

To provide a comprehensive and consistent evaluation of the proposed particle damper, the relationships among the three reported performance indices must be explicitly clarified. These metrics characterize the damping efficiency from different physical perspectives:

(1) The 63.24% RMS reduction evaluates the continuous dynamic stability of the actuator. Derived from the steady-state 30 Hz harmonic test, it represents the attenuation of the time-averaged vibration energy over operational cycles.
(2) The 67.5% peak reduction, extracted from the time-domain transient waveform, defines the damper's immediate capability to suppress the maximum instantaneous shock amplitude under the same continuous excitation.
(3) The 72.0% amplitude attenuation serves as a frequency-domain metric, specifically evaluating the maximum resonance suppression capability at the critical 70 Hz natural frequency during the broadband sweep test.

Together, these three complementary indices confirm that the optimized particle damper effectively mitigates instantaneous shocks, continuously reduces steady-state vibration energy, and rigorously suppresses worst-case resonant amplifications.

6. Conclusions

Aiming at the problem of low-frequency micro-vibration interference that restricts the positioning accuracy and dynamic stability of slender cantilever precision positioning actuators, this paper proposes an optimized particle damping passive vibration suppression method. The enhancement of structural anti-vibration performance contributes to suppressing environmental micro-vibration excitation responses and enhances the operational stability of high-precision positioning mechanisms. The main conclusions and innovative findings of this study are summarized as follows:

(1) A dynamic model of the slender cantilever precision positioning mechanism is established, and the structural natural frequencies and mode shapes are obtained through modal analysis. Based on the harmonic response and vibration transmission path analysis, the vibration-sensitive area at the cantilever terminal is determined as the optimal damper installation position, and the structural acceleration response characteristics within the main vibration band are clarified, providing a theoretical basis for the damper design.
(2) The parametric influence laws of particle dampers under low-frequency micro-vibration are revealed. Both particle size (0.5–2.0 mm) and filling ratio (65–98%) present a consistent unimodal variation trend for damping energy dissipation. Too small or overly large particle sizes and unreasonable filling ratios will restrict particle friction and collision behavior, reducing the damping efficiency. There exists a unique optimal parameter combination to maximize the energy dissipation capacity of the confined particle damper structure.
(3) Combined with numerical simulation and experimental verification, the best performing damper parameters among the tested discrete groups are determined as a 1.4 mm stainless steel particle size and 92% filling ratio. Compared with the original structure without a damper, the optimized particle damper achieves a terminal vibration damping rate of 63.24% and a peak acceleration attenuation of 67.5%. The high consistency between simulation and experimental results supports the reliability and effectiveness of the optimized damping scheme.
(4) The optimally configured particle damper possesses favorable broadband vibration suppression performance in the frequency range of 10–100 Hz. The matched particle

size and filling ratio balance particle motion space and contact density, activating micro-friction and collision energy dissipation. The damping performance peaks at the structural resonant frequency of 70 Hz, achieving efficient resonance suppression. This proposed method demonstrates good working adaptability, providing a valuable technical reference for the practical engineering application of particle damping in precision actuation systems.

Author Contributions: Conceptualization, B.W. and H.W.; methodology, H.W.; software, B.W.; validation, H.W., C.Z. and X.J.; formal analysis, B.W. and H.W.; investigation, C.Z.; resources, H.W.; data curation, H.D.; writing—original draft preparation, B.W.; writing—review and editing, L.Z.; visualization, M.L.; supervision, H.W.; project administration, H.W.; funding acquisition, B.W. All authors have read and agreed to the published version of the manuscript.

Funding: This research was financially supported by the Horizontal Cooperation Project between Changchun University of Science and Technology and Enterprise (Grant No. STC24A124) and the Science and Technology Development Project of Changchun University of Science and Technology (Grant No. WDZC2024JJ005). The APC was funded by Changchun University of Science and Technology.

Institutional Review Board Statement: Not Applicable.

Informed Consent Statement: Not Applicable.

Data Availability Statement: The data presented in this study are available on request from the corresponding author (Hao Wang). The data are not publicly available due to the continuity of the research project.

Acknowledgments: The authors gratefully acknowledge the strong support from Changchun University of Science and Technology, and thank all schoolmates in the Robot Intelligent Manufacturing Laboratory for their assistance in experiments and data collection.

Conflicts of Interest: The authors declare no conflicts of interest. The funders had no role in the design of the study; in the collection, analyses, or interpretation of data; in the writing of the manuscript; or in the decision to publish the results.

References

1. Zhang, Z.; Li, Q.; Zhang, Z.; Liu, L.; Li, W. Integrated modeling and active suppression of multi-source micro-vibrations in aerospace vehicles. *Adv. Space Res.* **2026**, *77*, 3670–3683. [CrossRef]
2. Long, Z.; Shen, H.; Zhang, J.; Zhao, S.; Lin, Y.; Li, Z. Dynamics Model and Vibration Control of Piezoelectric Feeder in Semiconductor Manufacturing Assembly. *IEEE Trans. Semicond. Manuf.* **2018**, *31*, 97–107. [CrossRef]
3. Lin, W.; Zhu, J.; Liu, Z.; Pang, X.; Zhou, Y.; Cui, W.; Dong, Z. Target Alignment Method of Inertial Confinement Fusion Facility Based on Position Estimation. *Nucl. Eng. Technol.* **2022**, *54*, 3703–3716. [CrossRef]
4. Zhu, M.; Wu, W.; Chen, X.; Chen, G.; Fu, X.; Du, Q.; Huang, Z.; Que, X.; Xu, Y.; Chen, X. Stability of Beam Positioning in ShenGuangIII. *Fusion Eng. Des.* **2018**, *126*, 36–43. [CrossRef]
5. Burnham-Fay, E.D. Vibration Stabilization of NIF-Scale Direct Drive Cryogenic Targets. Ph.D. Thesis, University of Rochester, Rochester, NY, USA, 2018.
6. Kundu, P.K.; Dhobale, S.M.; Chatterjee, S. Experimental Dynamic Modelling of a Nonlinear Cantilever Beam Using Adaptive Feedback Self-Excitation. *Mech. Syst. Signal Proc.* **2025**, *237*, 113131. [CrossRef]
7. Verma, A.K.; Saini, P.K. Use of Viscoelastic Material and Design Parameter Optimization for Optimum Reduction of Vibration Response of Primary System. *Mater. Today Proc.* **2022**, *71*, 259–264. [CrossRef]
8. Freundlich, J. Transient Vibrations of a Fractional Kelvin-Voigt Viscoelastic Cantilever Beam with a Tip Mass and Subjected to a Base Excitation. *J. Sound Vibr.* **2019**, *438*, 99–115. [CrossRef]
9. Qian, F.; Zuo, L. Tuned Nonlinear Spring-Inerter-damper Vibration Absorber for Beam Vibration Reduction Based on the Exact Nonlinear Dynamics Model. *J. Sound Vibr.* **2021**, *509*, 116246. [CrossRef]
10. Ozturk, B.; Cetin, H.; Dutkiewicz, M.; Aydin, E.; Noroozinejad Farsangi, E. On the Efficacy of a Novel Optimized Tuned Mass Damper for Minimizing Dynamic Responses of Cantilever Beams. *Appl. Sci.* **2022**, *12*, 7878. [CrossRef]

11. Song, H.; Shan, X.; Li, R.; Hou, C. Review on the Vibration Suppression of Cantilever Beam Through Piezoelectric Materials. *Adv. Eng. Mater.* **2022**, *24*, 2200408. [CrossRef]
12. Wang, M.; Jiang, Z.; Jiang, W.; Xianghui, F.; Jiheng, D.; Sun, Y.; Huayan, P.; Songquan, L. Active-Passive Vibration Control of Cantilever Beam Based on Magnetic Spring with Negative Stiffness and Piezoelectric Actuator. *Micromachines* **2025**, *16*, 1307. [CrossRef] [PubMed]
13. Amir, E.; Amir, O. Free Form Shape Optimization of Three Dimensional Beams Using Cross Section Analysis. *Int. J. Solids Struct.* **2023**, *277*, 112331. [CrossRef]
14. Nikaein, G.; Mohammadvali, M.H.; Sadeghi, M.H. Topology Optimization of Cantilever Beams with Non-Cellular, Cellular, and Hybrid Structures for Enhanced Mechanical Performance. *Appl. Eng. Sci.* **2026**, *25*, 100279. [CrossRef]
15. Sánchez, M.; Carlevaro, C.M. Nonlinear Dynamic Analysis of an Optimal Particle Damper. *J. Sound Vibr.* **2013**, *332*, 2070–2080. [CrossRef]
16. Shah, B.M.; Pillet, D.; Bai, X.M.; Keer, L.M.; Wang, Q.J.; Snurr, R.Q. Construction and Characterization of a Particle-Based Thrust Damping System. *J. Sound Vibr.* **2009**, *326*, 489–502. [CrossRef]
17. Heckel, M.; Sack, A.; Kollmer, J.E.; Pöschel, T. Granular Dampers for the Reduction of Vibrations of an Oscillatory Saw. *Physica A* **2012**, *391*, 4442–4447. [CrossRef]
18. Meyer, N.; Seifried, R. Toward a Design Methodology for Particle Dampers by Analyzing Their Energy Dissipation. *Comput. Part. Mech.* **2020**, *8*, 681–699. [CrossRef]
19. Xiao, W.; Huang, Y.; Jiang, H.; Jin, L. Effect of Powder Material on Vibration Reduction of Gear System in Centrifugal Field. *Powder Technol.* **2016**, *294*, 146–158. [CrossRef]
20. Ehlers, T.; Tatzko, S.; Wallaschek, J.; Lachmayer, R. Design of Particle Dampers for Additive Manufacturing. *Addit. Manuf.* **2021**, *38*, 101752. [CrossRef]
21. Lei, X.; Wu, C. Investigating the Optimal Damping Performance of a Composite Dynamic Vibration Absorber with Particle Damping. *J. Vib. Eng. Technol.* **2018**, *6*, 503–511. [CrossRef]
22. Hu, Y.; Zan, H.; Guo, Y.; Jiang, J.; Xia, Z.; Wen, H.; Peng, Z. Energy Dissipation Characteristics of Particle Dampers with Obstacle Grids. *Mech. Syst. Signal Proc.* **2023**, *193*, 110231. [CrossRef]
23. Zhao, C.; Shi, D.; Zheng, J.; Niu, Y.; Wang, P. New Floating Slab Track Isolator for Vibration Reduction Using Particle Damping Vibration Absorption and Bandgap Vibration Resistance. *Constr. Build. Mater.* **2022**, *336*, 127561. [CrossRef]
24. Xiao, W.; Xu, Z.; Wang, S.; Yu, S.; Qin, K.; Hu, D. Research on Vibration Reduction Characteristics of Continuum and Noncontinuum System on Coupling for High-Power Gear Transmission Based on Particle Damping Materials. *Shock Vib.* **2021**, *2021*, 8845526. [CrossRef]
25. Niedermeyer, J.; Ehlers, T.; Lachmayer, R. Potential of Additively Manufactured Particle Damped Compressor Blades: A Literature Review. *Procedia CIRP* **2023**, *119*, 570–575. [CrossRef]
26. Wang, W.; Li, Y.Y. Experimental Investigation on Vibration-Reduced Characteristics of Non-Obstructive Particle Damping for Free Beam Structure. *Adv. Mater. Res.* **2011**, *230–232*, 867–871. [CrossRef]
27. Prasad, B.B.; Duvigneau, F.; Reinboth, T.; Juhre, D.; Woschke, E. Design Strategies of Particle Dampers for Large-Scale Applications. *J. Vib. Eng. Technol.* **2023**, *12*, 5715–5746. [CrossRef]
28. Lu, Z.; Masri, S.F.; Lu, X. Studies of the Performance of Particle Dampers Attached to a Two-Degrees-of-freedom System under Random Excitation. *J. Vib. Control* **2011**, *17*, 1454–1471. [CrossRef]
29. Darabi, B.; Rongong, J.A. Polymeric Particle Dampers under Steady-State Vertical Vibrations. *J. Sound Vibr.* **2012**, *331*, 3304–3316. [CrossRef]
30. Lu, Z.; Masri, S.F.; Lu, X. Parametric Studies of the Performance of Particle Dampers under Harmonic Excitation. *Struct. Control Health Monit.* **2011**, *18*, 79–98. [CrossRef]
31. Xiao, W.; Yu, S.; Liu, L.; Zhang, F. Vibration Reduction Design of Extension Housing for Printed Circuit Board Based on Particle Damping Materials. *Appl. Acoust.* **2020**, *168*, 107434. [CrossRef]
32. Meyer, N.; Seifried, R. Numerical and Experimental Investigations in the Damping Behavior of Particle Dampers Attached to a Vibrating Structure. *Comput. Struct.* **2020**, *238*, 106281. [CrossRef]
33. Paulsen, T.T.; Coppotelli, G.; Santos, I.F. Remarks on the Effects of the Boundary Conditions on the Accuracy of the Estimate of the Modal Parameters in Operational Modal Analysis. *J. Braz. Soc. Mech. Sci. Eng.* **2025**, *47*, 574. [CrossRef]
34. Gordon, C.G. Generic vibration criteria for vibration-sensitive equipment. In *Optomechanical Engineering and Vibration Control*; Derby, E.A., Vukobratovich, D., Yoder, P.R., Zweben, C., Eds.; SPIE: Bellingham, WA, USA, 1999; Volume 3786, pp. 22–33. [CrossRef]

Disclaimer/Publisher's Note: The statements, opinions and data contained in all publications are solely those of the individual author(s) and contributor(s) and not of MDPI and/or the editor(s). MDPI and/or the editor(s) disclaim responsibility for any injury to people or property resulting from any ideas, methods, instructions or products referred to in the content.